Ph.D. Dissertation of Euijin Chang

# Whole Genome Sequencing and Mutational Analysis of SARS-CoV-2 in Immunocompromised Patients with Persistent Viral Detection

## SARS-CoV-2가 지속적으로 검출되는 면역저하 환자에서 바이러스 전체 유전체 염기서열 및 돌연변이 분석

August 2023

Graduate School of Medicine
Seoul National University
Internal Medicine Major

Euijin Chang

Ph.D. Dissertation of Euijin Chang

# Whole Genome Sequencing and Mutational Analysis of SARS-CoV-2 in Immunocompromised Patients with Persistent Viral Detection

SARS-CoV-2가 지속적으로 검출되는 면역저하 환자에서
바이러스 전체 유전체 염기서열 및 돌연변이 분석

August 2023

Graduate School of Medicine
Seoul National University
Internal Medicine Major

Euijin Chang

Confirming the Ph.D. Dissertation written by
Euijin Chang

August 2023

| | |
|---|---|
| Chair | Eun Hwa Choi |
| Vice Chair | Hong Bin Kim |
| Examiner | Nam Joong Kim |
| Examiner | Wan Beom Park |
| Examiner | Sung-Han Kim |

# Abstract

**Background:** Since the emergence of Severe Acute Respiratory Syndrome-Coronavirus-2 (SARS-CoV-2) in December 2019, several variants of interest (VOIs) and variants of concern (VOCs) have evolved. SARS-CoV-2 can persist in immunocompromised patients, acquiring new mutations that could give rise to new variants, enable immune evasion, or promote treatment resistance. Therefore, monitoring these mutations becomes crucial to understanding their dynamics, characteristics, and clinical impacts. Most previous studies focused on mutations associated with immune evasion during the pre-Omicron era and included only a few immunocompromised patients. Thus, there is a need for more comprehensive research during the Omicron era. This study was designed to investigate the characteristics of nonsynonymous mutations acquired in SARS-CoV-2 genomes among immunocompromised patients during the Omicron-prevalent period.

**Methods:** From February to November 2022, we conducted a prospective study involving immunocompromised adults diagnosed with SARS-CoV-2. Whenever possible, we collected saliva, sputum, and blood samples on a weekly basis for genomic and antibody testing.

We measured the amount of SARS-CoV-2 RNA through polymerase chain reaction (PCR) and performed viral cultures on specimens with positive real-time reverse transcription PCR results to check for viable virus shedding. We selected respiratory samples for whole-genome sequencing (WGS) to identify and classify nucleotide polymorphisms resulting in new mutations. We also carried out a literature review to determine whether these mutations were associated with immune evasion, remdesivir resistance, or other SARS-CoV-2 variants. Additionally, we used the collected blood samples to measure the titers of neutralizing antibodies against SARS-CoV-2 Omicron variants by the plaque reduction neutralization test.

**Results:** The final analysis included thirteen patients, of whom eleven (84.6%) had hematologic malignancies, and two (15.4%) were recipients of solid organ transplants. Nearly half (46.2%) had been treated with B cell-depleting agents within two years prior to their SARS-CoV-2 diagnosis, and only two patients (15.4%) had received at least three doses of a SARS-CoV-2 vaccine. Notably, the majority (69.2%) were found to be infected with the BA.2 or BA.2.3 sub-lineages of the virus, as determined through WGS analysis.

Each immunocompromised patient underwent WGS analysis

a median of three times, with a median interval of 20 days between consecutive analyses, and a span of 51 days between the first and last analyses. Patients acquired a median of two nonsynonymous mutations, which were dispersed across the entire viral genome.

Among the 87 nonsynonymous mutations, 16 (18.4%) and 13 (14.9%) were classified as persistent and temporary mutations respectively, with the majority located in the ORF1ab region. In the spike region, 28 mutations were identified, with 12 associated with immune evasion and 11 designated as the defining mutations of other SARS-CoV-2 variants, including Omicron subvariants such as BA.1, BA.4, BA.5, BA.2.75, XBB, and XBB.1.5. The proportion of the defining mutations of other variants was higher in the spike region compared to the entire genome (39.3% vs. 14.9%).

The mutation ORF1ab:V5184I, reported to be associated with decreased sensitivity to remdesivir, was observed in patient H, 142 days after the initial SARS-CoV-2 diagnosis. This patient had undergone multiple treatment cycles with remdesivir, dexamethasone, and baricitinib, and received high-dose steroids for over two months prior to this mutation.

Patient J, despite having a high titer of neutralizing antibodies, continued to shed the virus. This might be potentially attributed to a missense mutation, S:L452Q, which is reported to be associated with

immune evasion and decreased antibody sensitivity. This mutation might enable persistent viral shedding, even in the presence of high-titer neutralizing antibodies.

**Conclusions:** Several new mutations reported to be associated with immune evasion, remdesivir resistance, and new Omicron subvariants such as BA.2.75, BA.4, BA.5, BQ.1, and XBB, emerged in the SARS-CoV-2 genomes of immunocompromised patients with persistent viral detection during the Omicron-prevalent era. Regarding the emergence of new strains with mutations reported to be related to immune evasion or remdesivir resistance and the possibility of shedding viable viruses from immunocompromised individuals, decisions to end the isolation of immunocompromised patients with SARS-CoV-2 infection should be made with caution.

**Keywords:** Severe Acute Respiratory Syndrome-Coronavirus-2, immunocompromised, whole-genome sequencing, nonsynonymous mutation, immune evasion, remdesivir resistance, variant of concern

**Student Number:** 2021-30823

# Table of Contents

# Tables

# Figures

# Chapter I. Introduction

## 1. Current status of the COVID-19 epidemic and the emergence of variants

Since December 2019, when Severe Acute Respiratory Syndrome-Coronavirus-2 (SARS-CoV-2) first appeared in Wuhan, China, there have been about 760 million confirmed cases of Coronavirus disease-19 (COVID-19) and 6.9 million deaths all over the world, as of 12 April 2023 [1]. For more than three years during the COVID-19 pandemic, several variants of being monitored (VBMs), of interest (VOIs), and of concern (VOCs) evolved from the previous prevalent variants [2]. The Delta variant first appeared in India and dominated in almost every country by late 2021, acquiring new spike mutations such as S:L452R and S:P681R that impact antibody binding [3]. Next, the Omicron variant emerged in November 2021 in South Africa and has been prevalent all over the world to the present. Specific mutations at the S1-S2 furin cleavage site conferred rapid transmissibility on this variant [3], and new subvariants including BA.2.75, BQ.1, XBB, and XBB.1.5 have evolved recently from the

previous Omicron subvariants [4]. These new subvariants also exhibited greater immune evasion and enhanced infectivity by the acquisition of further mutations or inter-lineage recombination [5,6].

## 2. Accumulation of various mutations in the SARS-CoV-2 genomes in specimens from immunocompromised patients

SARS-CoV-2 can be cultured for more than several months in severely immunosuppressed patients infected with COVID-19 and various mutations accumulate in the SARS-CoV-2 genomes in the respiratory specimens from the immunocompromised. One patient, who received rituximab and bendamustine treatments six times each in 2016 and 2020 due to lymphoma, was diagnosed with COVID-19 in November 2020. SARS-CoV-2 viral RNA was detected in her respiratory specimens for six months afterward, and it was observed that mutations associated with immune escape in variants of concern, such as S:E484K, S:D950N, S:P681H, S:N501Y, and S:H655Y, accumulated in the virus genomes [7]. Another patient, who had recurrent acute lymphoblastic leukemia after hematopoietic stem cell transplant and received several doses of immunosuppressants, also shed the virus for 78 days after being infected with COVID-19.

During this period, several mutations like S:Y144del, S:F490L, and S:S494P accumulated in the SARS-CoV-2 genomes [8].

Moreover, mutations associated with resistance to remdesivir, such as nsp12 E802D and nsp12 V792I, appeared in the specimens from the immunocompromised patients who received remdesivir after diagnosis of COVID-19 [9,10]. Also, mutations like nsp12 V792I and nsp12 S759A appeared in the SARS-CoV-2 genomes when SARS-CoV-2 was repeatedly cultured in vitro, and the half-maximal effective concentration of remdesivir against SARS-CoV-2 with these mutations increased by more than 3-10 times [11].

## 3. The limitations of previous studies and necessities of further studies

As described above, SARS-CoV-2 viruses can reside in immunocompromised patients for several months and more, and acquire new mutations associated with new variants, immune evasion, or resistance to treatments as a result of selective pressures exerted by antiviral and immunomodulatory treatments and therapeutic antibodies [7-18]. Therefore, it could be helpful to monitor the acquisition of new mutations in the SARS-CoV-2 genomes from

immunocompromised patients, because this could enhance our understanding of the dynamics, characteristics, and clinical impacts of new mutations.

Previous studies were conducted mainly during the pre-Omicron era, which detected the immune escape mutations defining the Beta, Delta, or Omicron variants, by whole-genome sequencing (WGS), and included only a few immunocompromised patients [7,13-15,19-23]. This warrants the study performed during the Omicron era including a larger number of immunocompromised patients.

Furthermore, previous research has focused on immune evasion by newly-acquired mutations in the SARS-CoV-2 genome [14,24-31]. Additionally, there have been a few reports detailing the occurrence and incidence of resistance to remdesivir following prolonged therapy for SARS-CoV-2 infection [9,10]. Remdesivir, an adenosine nucleoside analog, inhibits SARS-CoV-2 RNA-dependent RNA polymerase (RdRp) to suppress viral replication and has been widely used in the prevention and treatment of COVID-19 pneumonia [32]. The incidence of resistance to remdesivir in SARS-CoV-2 has not been clearly determined, and some reports suggested that resistance to remdesivir hardly arises [33,34]. Therefore, mutations not only associated with immune evasion but also with remdesivir resistance should be investigated in further studies.

## 4. Goals and hypotheses of the present study

We conducted the present study using WGS analyses to investigate the characteristics of nonsynonymous SARS-CoV-2 mutations that have arisen in immunocompromised patients with persistent viral detection during the Omicron-prevalent era. We also aimed to identify newly-acquired mutations reported to be associated with immune evasion, remdesivir resistance, and the new Omicron subvariants.

We anticipated that new nonsynonymous mutations associated with immune evasion or resistance to remdesivir might emerge in the SARS-CoV-2 genomes detected in immunocompromised patients. Likewise, during the Omicron-prevalent era, we expected to find the mutations characteristic of the new Omicron subvariants in the SARS-CoV-2 genomes from immunosuppressed individuals.

# Chapter II. Methods

## 1. Study participants and specimen collection

This prospective study was conducted at the Asan Medical Center (AMC), a 2,732 bed-tertiary teaching hospital, from February to November 2022. Following the definition of "immunocompromised" by the Centers for Disease Control and Prevention [35], we enrolled immunocompromised adults (age ≥ 18 years) who had hematologic malignancies or received solid organ transplants and were within 12 weeks from the initial diagnosis of SARS-CoV-2 infection. All the patients were confirmed to have SARS-CoV-2 infections by nasopharyngeal swab polymerase chain reaction (PCR), and patients with a history of prior SARS-CoV-2 infection were excluded.

We obtained nasopharyngeal swabs, saliva, and blood samples weekly from the enrolled patients. SARS-CoV-2 loads were measured in each saliva sample and nasopharyngeal swab by genomic RNA real-time reverse transcription-PCR (RT-PCR), and those with positive results were cultured to detect persistent viral shedding. Also, at least two or more respiratory specimens with a cycle threshold value of less than 30 were selected for SARS-CoV-

2 WGS for each patient. Blood samples were used to measure neutralizing antibodies against SARS-CoV-2 omicron variants.

Clinical information on the study participants, including age, sex, comorbidities, history of vaccination against SARS-CoV-2, and treatments for SARS-CoV-2 infection was reviewed in electronic medical records, and written informed consent was obtained from the participants. This study was approved by the institutional review boards of the AMC (IRB-2022-1054).

## 2. Measurement of SARS-CoV-2 RNA

PCR reaction mixtures (20 μL) contained 5 μL of extracted RNA or in vitro-synthesized control RNA, 500 and 200 nM of S gene primers and probes, 500 and 250 nM of N gene primers and probes, 250 and 125 nM of internal control primers and probes respectively, 0.1 μL of 200× enzyme mix, and 4 μL of 5× master mix (LightCycler Multiplex RNA Virus Master, Roche, Basel, Switzerland) (Table 1).

RNA amplification was performed using a LightCycler 96 system (Roche) as follows; (i) reverse transcription at 50℃ for 10 minutes → (ii) initial denaturation at 95℃ for 5 minutes → (iii) 45 cycles of 2-step amplification → (iv) denaturation at 95℃ for 10

seconds → (v) annealing and elongation at 60℃ for 30 seconds → (vi) final extension at 60℃ for 5 minutes.

We generated calibration curves by conducting six independent assays with samples of synthetic control RNA serially diluted from $5\times10^{7}$ to $5\times10^{1}$ copies/$\mu$L. The limit of detection in this assay was 5 copies/reaction (2.6 log copies/ml of specimen), and viral copy numbers were calculated by plotting Ct values of the SARS-CoV-2 N gene against log copies/reaction [36].

Table 1. Primers and probes used in real-time RT-PCR assays to detect the N and S genes of SARS-CoV-2[a]

| Target (Accession #) | Name | Location | Sequence | Modification |
|---|---|---|---|---|
| N gene (NC_045512) | NF | 29356 | AACATTCCCACCAACAGAGC | |
| | NR | 29529 | GCCTGAGTTGAGTCAGCACT | |
| | NP | 29462 | GCTGATGAAACTCAAGCCTTACCGCA | 5' Cy5, 3' BHQ2 |
| S gene (NC_045512) | SF | 21624 | GAACTCAATTACCCCCTGCAT | |
| | SR | 21787 | ACCATTGGTCCCAGAGACAT | |
| | SP | 21657 | TCACACGTGGTGTTTATTACCCTGACA | 5' FAM, 3' BHQ1 |
| Internal control (NC_000007.14) | BAF | 1670 | ACTAACACTGGCTCGTGTGA | |
| | BAR | 1774 | CTTGGGATGGGGAGTCTGTT | |
| | BAP | 1700 | AGGCTGGTGTAAAGCGGCCTTGG | 5' HEX, 3' BHQ1 |

[a] The samples were considered positive for SARS-CoV-2 genomic RNA when PCR results for both N and S genes, as well as the internal control, were positive.

## 3. Culture of SARS-CoV-2

Respiratory specimens with positive SARS-CoV-2 RNA RT-PCR results were cultured to detect viable viruses in a biosafety level 3 (BSL3) facility. Culture for SARS-CoV-2 was performed as the previously described method [37,38]. Samples were inoculated into previously prepared Vero-E6 cells ($1.5 \times 10^5$ cells/well). The inoculated cells were incubated for 1 hour at 37℃ with 5% $CO_2$. After removal of the inoculum, the cells were incubated again with Dulbecco's modified Eagle's medium containing 2% fetal bovine serum and 1% penicillin-streptomycin.

Cytopathic effects in the infected cells were checked for one week. Supernatants from the infected cells were collected on the seventh day and the SARS-CoV-2 viral load was measured by real-time RT-PCR. The culture results were considered positive when the cytopathic effects in the inoculated cells were observed and SARS-CoV-2 viral loads in the supernatants exceeded $10^6$ copies/ml.

Culture tests were repeated in the case of the SARS-CoV-2 viral loads of less than $10^6$ copies/ml in the supernatants with cytopathic effects in the previously infected cells. The supernatants were inoculated again into other cells and incubation

was done as described above. Then, SARS-CoV-2 real-time RT-PCR was conducted to confirm virus viability, using the supernatants from these sub-passaged cells. The viral culture was considered positive when cytopathic effects were observed in the sub-passaged cells and SARS-CoV-2 RNA was detected in the supernatants from the sub-passaged cells.

## 4. Whole-genome sequencing and mutational analysis

Two or more respiratory samples, taken with an interval of at least two weeks and with Ct values below 30, were chosen from each patient for whole-genome sequencing. Viral nucleic acids were extracted using the automatic extraction instrument (Maxwell RSC 48 system, Promega, Madison, WI, USA). To isolate pure SARS-CoV-2 RNA, human RNA was removed from samples with a NEBNext rRNA Depletion Kit (New England Biolabs, Ipswich, MA, USA). Libraries were prepared with a TruSeq RNA sample preparation kit v2 (Illumina, San Diego, CA, USA). The enriched libraries were quantified using a Kapa Library Quantification Kit (Roche, Basel, Switzerland), and sequenced with a Miseq reagent kit v2 (300 cycles) (Illumina). Sequences were analyzed on a CLC

Genomics Workbench 10 (QIAGEN).

FASTQ files containing the raw reads were trimmed and mapped to the reference Wuhan-Hu-1 sequence (GeneBank accession number NC_045512.2). Viral genome assembly and variant calling for each genome were done with Multiple Alignments using Fast Fourier Transform (MAFFT), and pangolin lineages were identified with the Pangolin software, version 4.2 (https://pangolin.cog-uk.io/).

The most frequent single nucleotide polymorphisms resulting in new nonsynonymous mutations were detected by comparison with the SARS-CoV-2 genome in the initial sample from each patient. We classified acquired nonsynonymous mutations into three groups: (i) persistent mutations detected in at least two consecutive samples; (ii) temporary mutations that appeared only once and disappeared from subsequent samples; and (iii) undetermined mutations that occurred only in the last sample from a patient so that it was not known whether they were temporary or persistent [7]. Then, we investigated whether the identified nonsynonymous mutations were associated with immune evasion or resistance to remdesivir, referencing previous reports and studies. We also determined if these mutations were included in the defining mutations of the major SARS-CoV-2 variants, using the lists

provided by CoVariant.org [3].

## 5. Plaque reduction neutralization test (PRNT)

Neutralizing antibodies in blood were measured in a BSL3 facility. The live SARS-CoV-2 viruses used in this assay were Omicron variants BA.1 (hCoV-19/Korea/NCCP 43408/2021, EPI_ISL_2887353), BA.2 (hCoV-19/Korea/NCCP 43412/2022, EPI_ISL_13086512), and BA.5 (hCoV-19/Korea/NCCP 43426/2022, EPI_ISL_13086516) provided by the KDCA. When a patient was infected with the Omicron BA.1 lineage, the PRNT was conducted against Omicron BA.1, and similarly for the Omicron BA.2 and BA.5 lineages.

PRNT was performed as the previously described methods [39,40]. Serially diluted serum and an equal volume of virus (40 plaque-forming units per well) were mixed and incubated at 37℃ for two hours. Next, this mixture was inoculated into the 24-well plate with Vero E6 cells ($1 \times 10^5$ cells/well) and incubated at 37℃ for one hour. Then, 1 ml of 0.5% agarose (Lonza) was added to the plate. After two to three days of incubation, the cells were fixed with 4% paraformaldehyde and stained with crystal violet to visualize the plaques. Using the Spearman-Karber formula [41], the 50%

neutralization dose (ND50) of antibodies against SARS-CoV-2 was calculated, which resulted in a 50% reduction of plaques, and presented as the reciprocal of serum dilution.

## 6. Statistical analysis

Fisher's exact test was used to analyze categorical variables, and the Mann-Whitney U test or Student's t-test was performed for continuous variables, depending on whether the data were normally distributed or not. Two-tailed *p*-values less than 0.05 were considered statistically significant. We used R version 4.2.3 (R Foundation for Statistical Computing, Vienna, Austria) and GraphPad Prism version 9.0 (GraphPad Software, San Diego, California) for the analysis and presentation of the results.

# Chapter III. Results

## 1. Clinical characteristics of the study participants

We enrolled 17 patients during the study period and chose 66 samples from them for WGS. Four patients were excluded from the final analysis due to the poor quality of genomic data or the insufficient number of WGS results. Three of them had hematologic malignancies and the other patient received a kidney transplant. Therefore, at least two successive sets of whole-genome data from 13 SARS-CoV-2 patients were included in the final analysis without any selection bias (Figure 1).

The clinical characteristics of the study participants are summarized in Table 2. Two of the patients (15.4%) received solid organ transplants and the others had hematologic malignancies. Also, six of the patients (46.2%) had received B cell-depleting agents such as anti-CD20 monoclonal antibodies and bispecific T cell engagers within two years of the diagnosis of SARS-CoV-2 infection. Two patients (15.4%) had received at least three doses of Comirnaty® (Pfizer Inc., Manhattan, New York, United States), Spikevax® (Moderna Inc., Cambridge, Massachusetts, United States), or

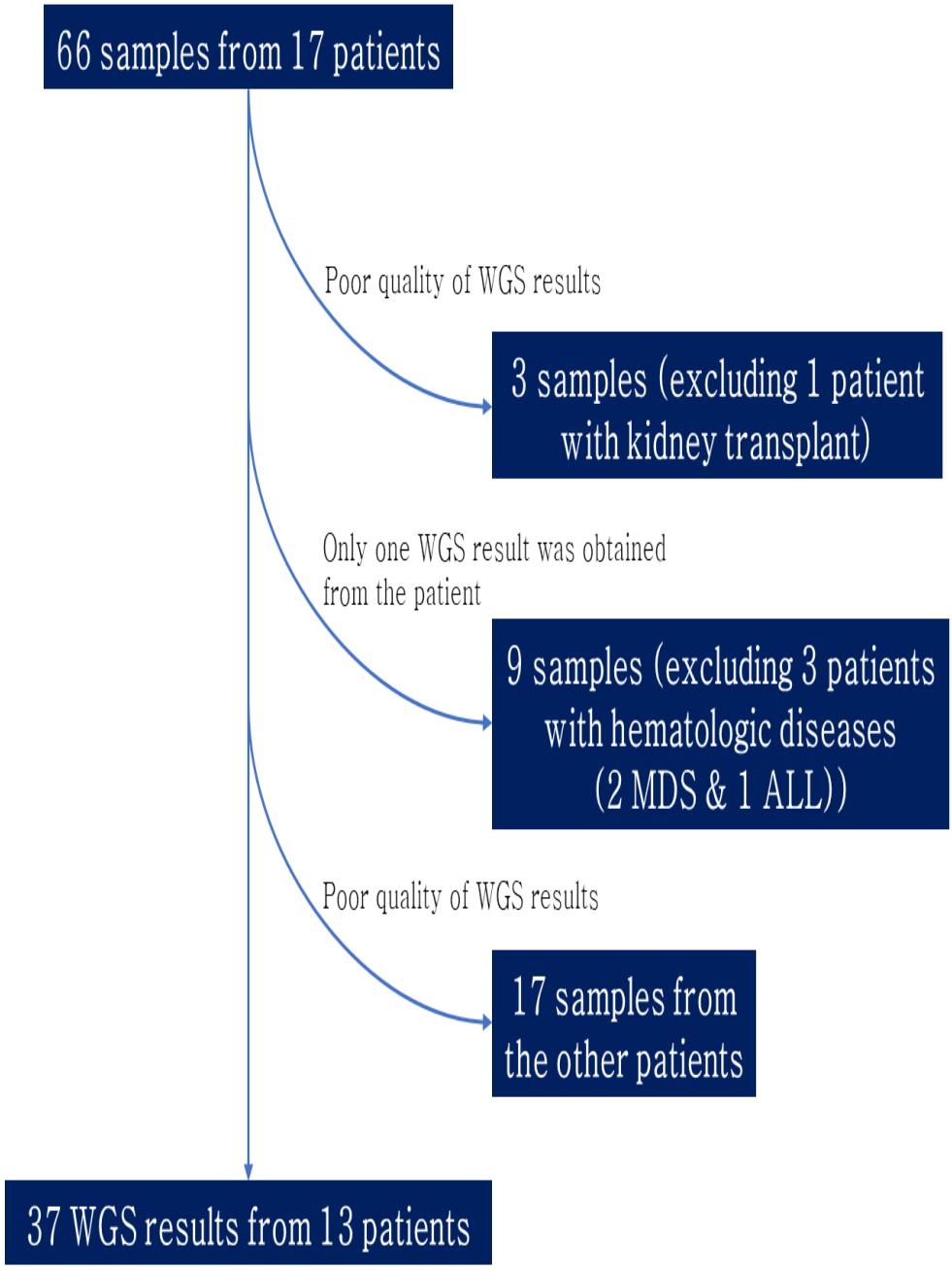


Figure 1. The flow diagram of the samples and patients included in the final analysis.

Abbreviations: WGS, whole-genome sequencing; MDS, myelodysplastic syndrome; ALL, acute lymphoblastic leukemia

Vaxzevria® (AstraZeneca Plc., Cambridge, United Kingdom) against SARS-CoV-2, while eight patients (61.5%) had not received any vaccine. All the patients received remdesivir after their diagnosis of SARS-CoV-2 infection, and immunomodulatory agents such as dexamethasone, baricitinib, or tocilizumab were administered to the patients depending on the severity of their infection [42]. Nine patients (69.2%) were identified as infected with the BA.2 or BA.2.3 sub-lineage by WGS analysis.

Table 2. Clinical characteristics of the immunocompromised patients

| Characteristic | Number (%) |
|---|---|
| Age (years), mean (±SD) | 55.8 (±9.0) |
| Male | 9 (69.2) |
| Immunocompromised condition | |
| Hematologic malignancy | 11 (84.6) |
| Acute myelogenous leukemia | 4 (30.8) |
| Acute lymphocytic leukemia | 1 (7.7) |
| Non-Hodgkin lymphoma | 6 (46.2) |
| Autologous SCT | 1 (7.7) |
| Allogeneic SCT | 5 (38.5) |
| Solid organ transplant | 2 (15.4) |
| kidney | 1 (7.7) |
| liver | 1 (7.7) |
| B cell-depleting agent[a] | 6 (46.2) |
| Comorbidity | |
| Diabetes mellitus | 2 (15.4) |
| Hypertension | 3 (23.1) |
| Chronic kidney disease | 1 (7.7) |
| Peripheral vascular disease | 1 (7.7) |
| Cerebrovascular accident | 1 (7.7) |
| Connective tissue disease | 3 (23.1) |
| Charlson comorbidity index, median (IQR) | 3 (3-4) |
| SARS-CoV-2 vaccination status | |
| None | 8 (61.5) |
| Partial[b] | 3 (23.1) |
| Full[c] | 2 (15.4) |
| Treatment for SARS-CoV-2 infection | |

| | |
|---|---|
| Remdesivir | 13 (100.0) |
| Dexamethasone | 6 (46.2) |
| Baricitinib | 4 (30.8) |
| Tocilizumab | 3 (23.1) |
| Tixagevimab−cilgavimab | 1 (7.7) |
| Nirmatrelvir/ritonavir | 2 (15.4) |
| Initial SARS−CoV−2 lineage | |
| BA.1.1 | 1 (7.7) |
| BA.2 | 5 (38.5) |
| BA.2.3 | 4 (30.8) |
| BA.2.3.11 | 1 (7.7) |
| BA.2.10 | 1 (7.7) |
| BA.5.2 | 1 (7.7) |

Abbreviations: SD, standard deviation; SCT, stem cell therapy; IQR, interquartile range; SARS−CoV−2, severe acute respiratory syndrome−coronavirus−2

[a] Use of anti−CD20 monoclonal antibodies or bispecific T cell engagers within two years

[b] One or two vaccinations against SARS−CoV−2 with Comirnaty®, Spikevax®, or Vaxzevria®

[c] More than two vaccinations against SARS−CoV−2 with Comirnaty®, Spikevax®, or Vaxzevria®

## 2. Acquisition of nonsynonymous SARS-CoV-2 mutations in immunocompromised patients

The results of WGS analysis were obtained from each immunocompromised patient with a median frequency of three times (interquartile range (IQR) 2-3). The median intervals between consecutive WGS analyses and between the first and last WGS analyses were 20 days (IQR 15-46 days) and 51 days (IQR 28-63 days), respectively. The time points at which WGS, viral PCR, or culture was conducted for each patient are detailed in Figure 2.

The patients acquired a median of two nonsynonymous mutations (IQR 1-7), excluding temporary mutations. The specific nonsynonymous mutations compared with the Wuhan Hu-1 reference genome and the acquired nonsynonymous mutations detected in subsequent WGS analyses are presented for each patient in Figure 3 and Table 3. Table 4 outlines the number of nonsynonymous mutations associated with immune evasion and the defining mutations of the major variants for each patient.

The mutations each patient acquired were sporadically distributed across the entire regions of the viral genome. Notably, there were changes in the Pangolin lineages of the detected viruses in the specimens from patients B and C. For patient B, the SARS-

CoV−2 lineage shifted from BA.2 to BA.2.68, 79 days after the initial diagnosis. Patient C initially showed the BA.2.10 lineage, which then changed to BA.2 on the 19th day after the initial diagnosis, only to revert back to BA.2.10 on the 34th day. Despite these shifts, all of the viruses detected in patients B and C belonged to the 21L Nextstrain clade, with no observed change in the clade [43,44]. Additionally, no alterations in the SARS−CoV−2 lineages were found among the other patients. Figure 3 further presents the results of viral cultures for each specimen. The acquisition of new mutations was observed in specimens yielding both negative and positive results from viral culture.

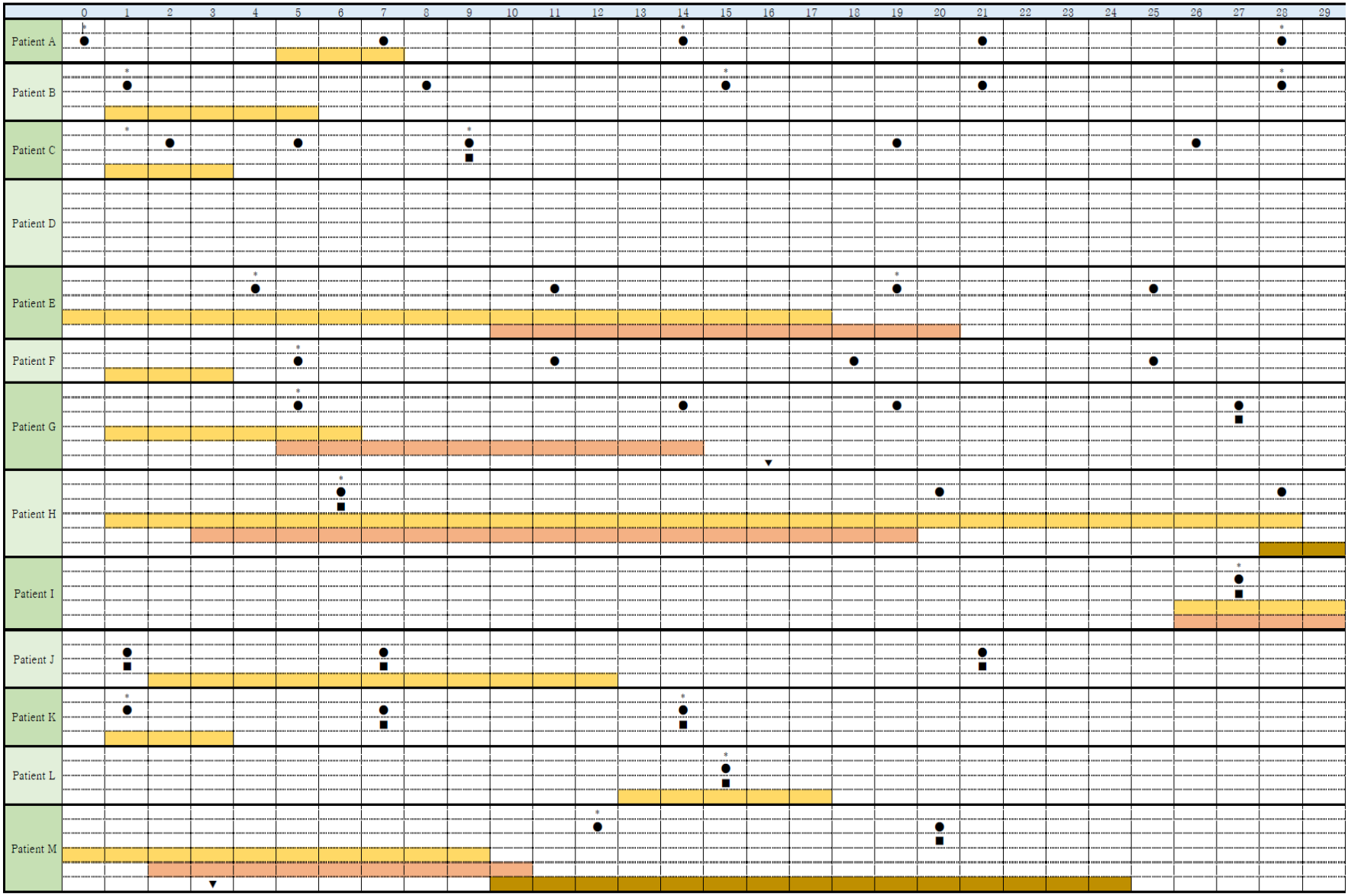
0 1 2 3 4 5 6 7 8 9 10 11 12 13 14 15 16 17 18 19 20 21 22 23 24 25 26 27 28 29
Patient A
Patient B
Patient C
Patient D
Patient E
Patient F
Patient G
Patient H
Patient I
Patient J
Patient K
Patient L
Patient M

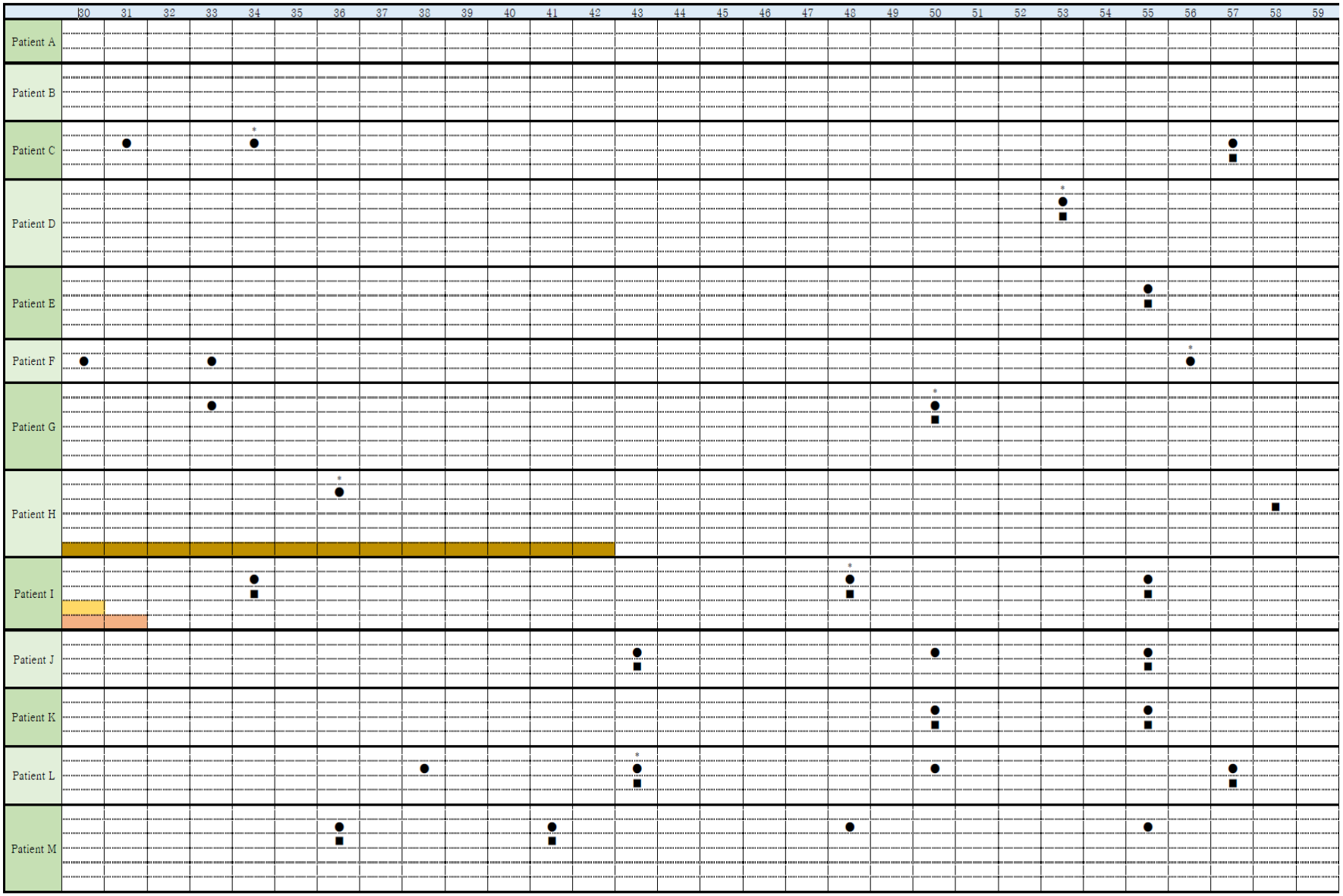
30
31
32
33
34
35
36
37
38
39
40
41
42
43
44
45
46
47
48
49
50
51
52
53
54
55
56
57
58
59
Patient A
Patient B
Patient C
Patient D
Patient E
Patient F
Patient G
Patient H
Patient I
Patient J
Patient K
Patient L
Patient M

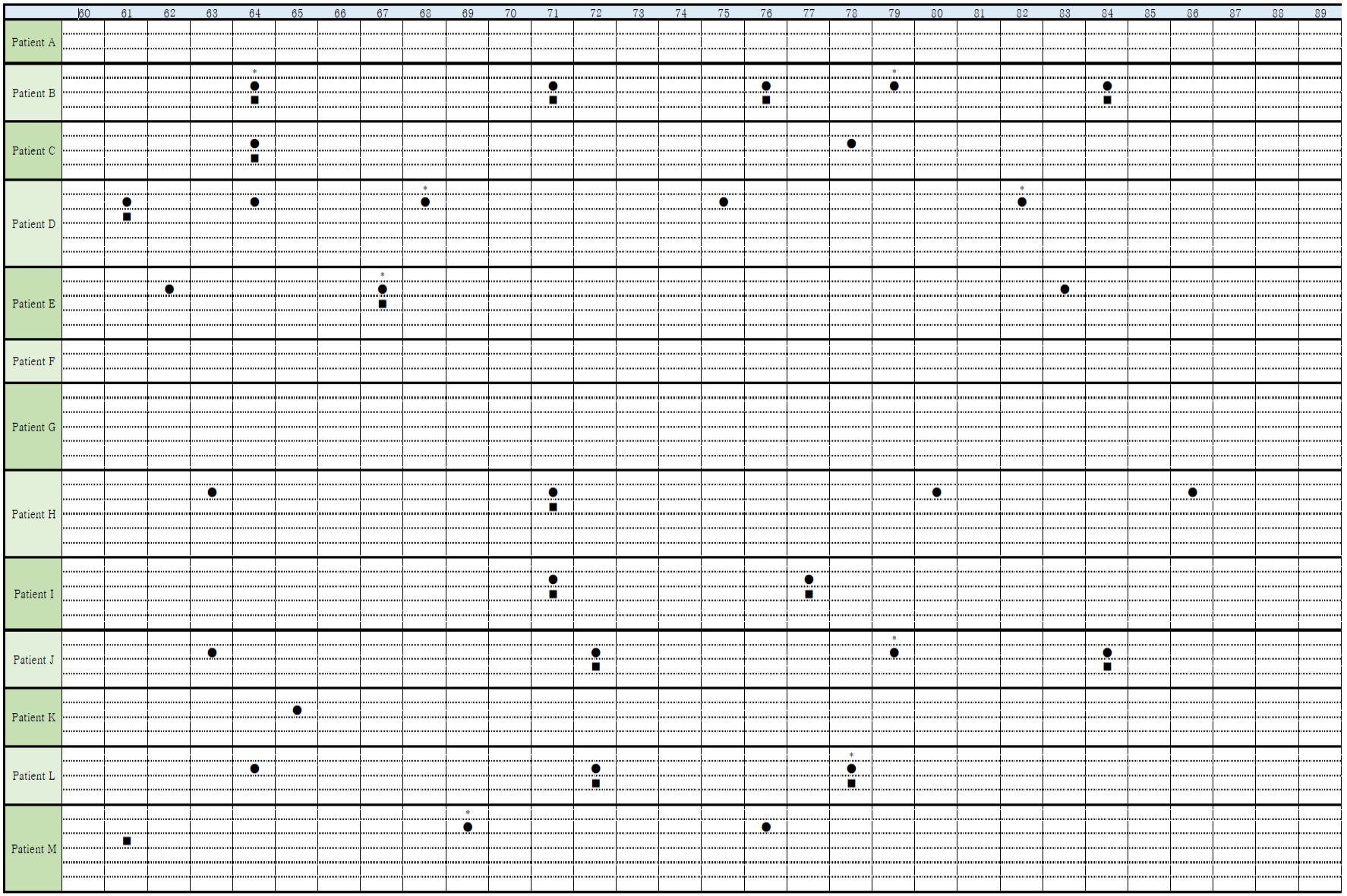
60
61
62
63
64
65
66
67
68
69
70
71
72
73
74
75
76
77
78
79
80
81
82
83
84
85
86
87
88
89
Patient A
Patient B
Patient C
Patient D
Patient E
Patient F
Patient G
Patient H
Patient I
Patient J
Patient K
Patient L
Patient M

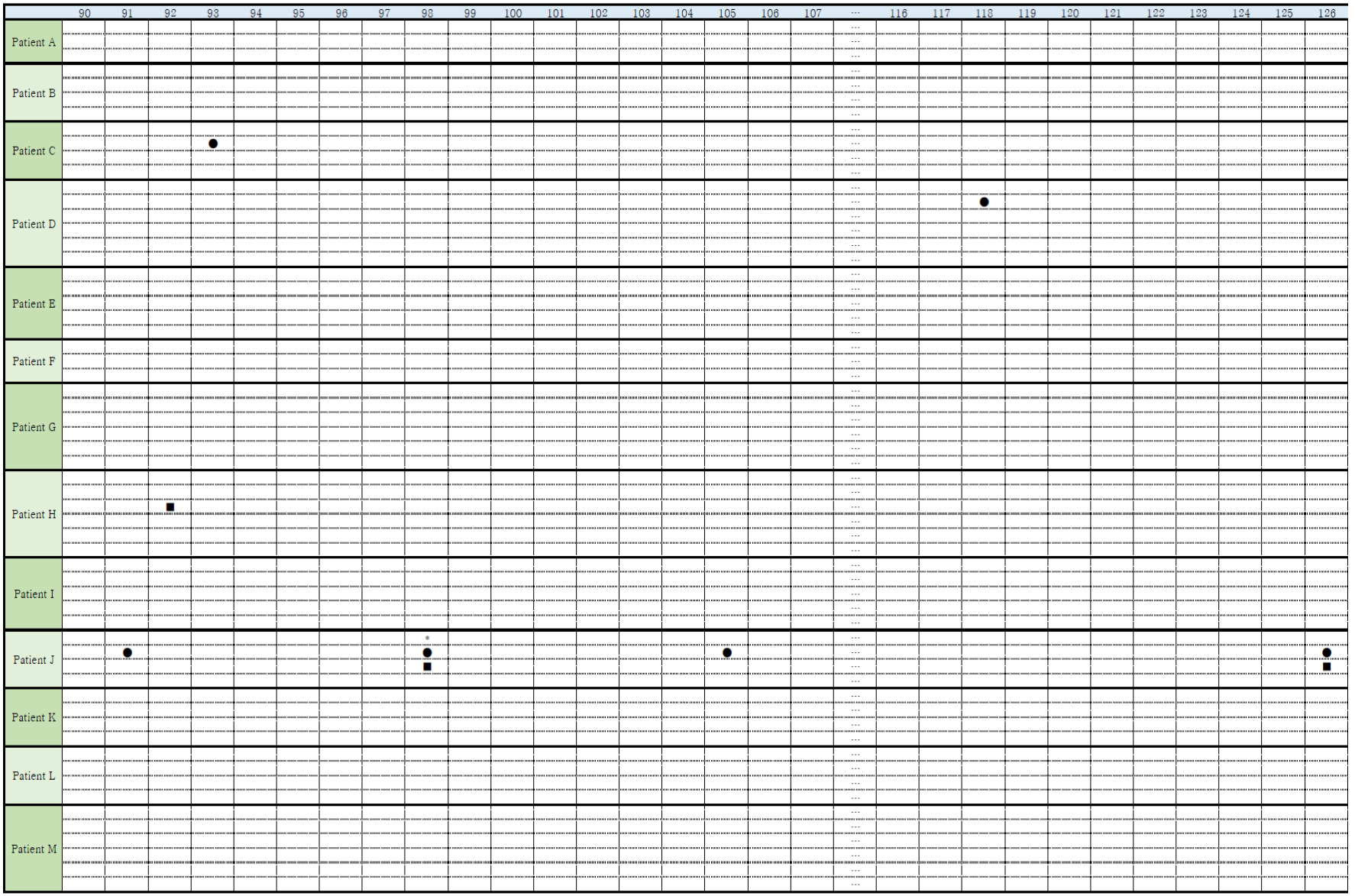
90
91
92
93
94
95
96
97
98
99
100
101
102
103
104
105
106
107
116
117
118
119
120
121
122
123
124
125
126
Patient A
Patient B
Patient C
Patient D
Patient E
Patient F
Patient G
Patient H
Patient I
Patient J
Patient K
Patient L
Patient M

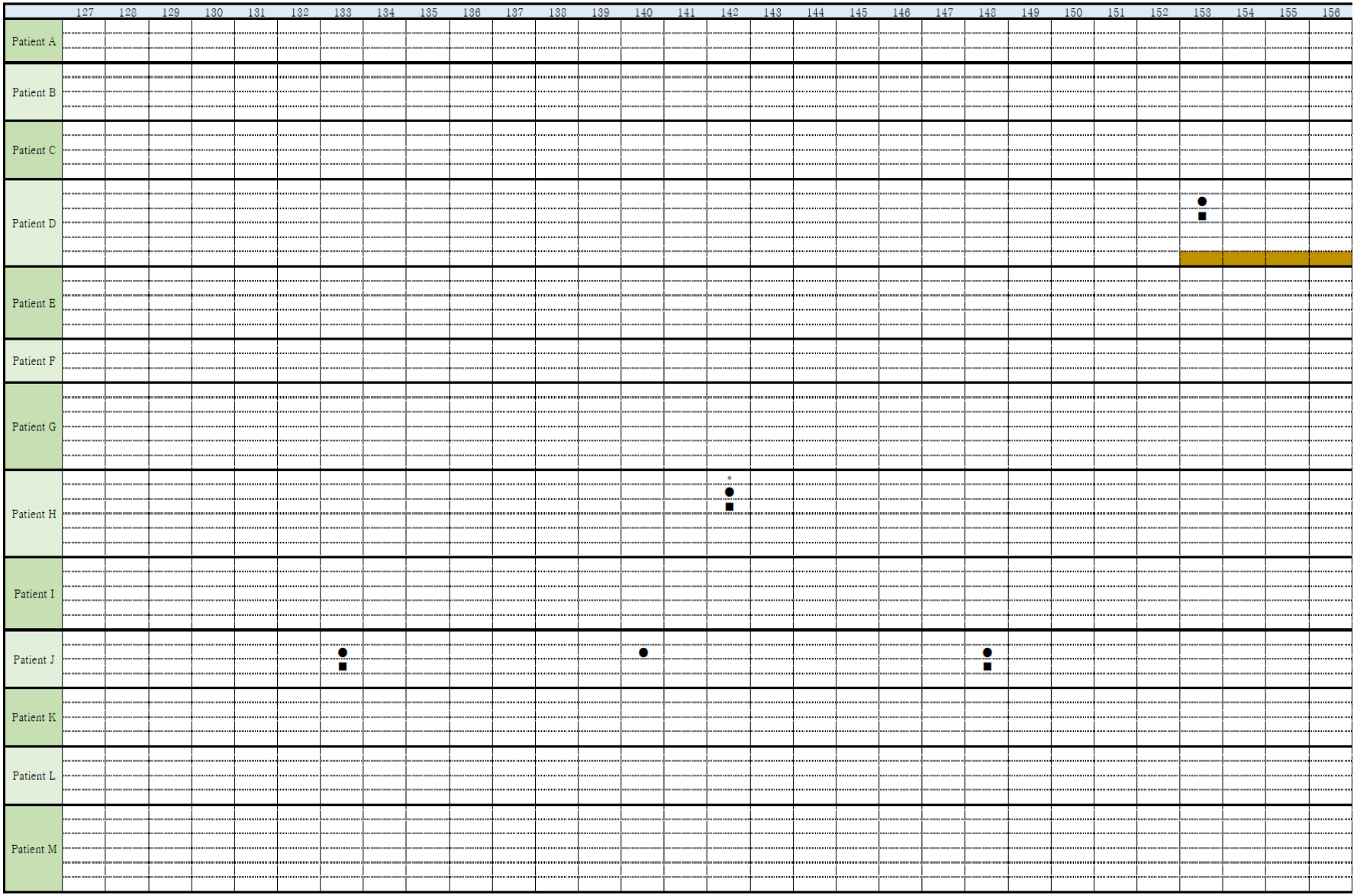
127 128 129 130 131 132 133 134 135 136 137 138 139 140 141 142 143 144 145 146 147 148 149 150 151 152 153 154 155 156
Patient A
Patient B
Patient C
Patient D
Patient E
Patient F
Patient G
Patient H
Patient I
Patient J
Patient K
Patient L
Patient M

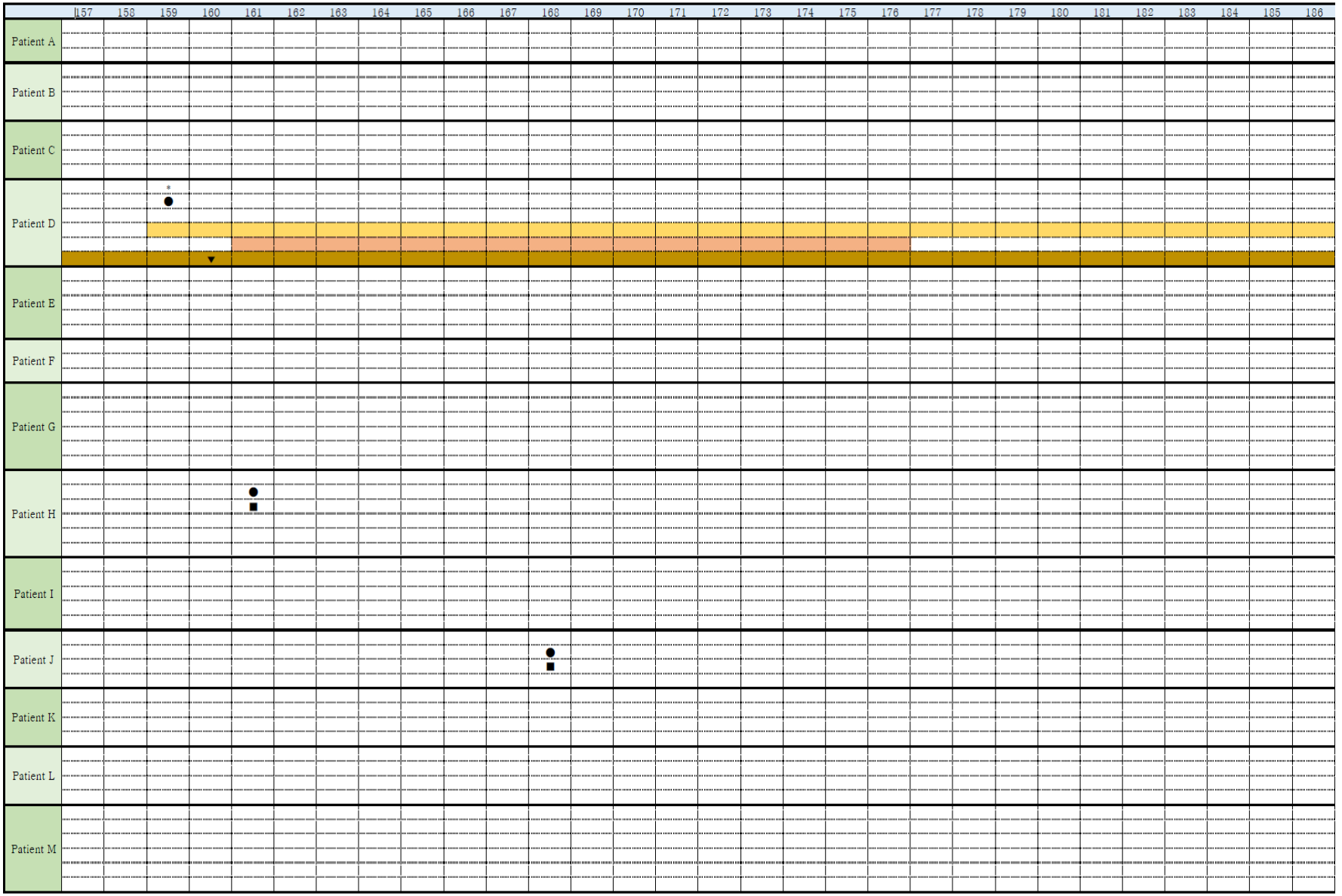
157
158
159
160
161
162
163
164
165
166
167
168
169
170
171
172
173
174
175
176
177
178
179
180
181
182
183
184
185
186
Patient A
Patient B
Patient C
Patient D
Patient E
Patient F
Patient G
Patient H
Patient I
Patient J
Patient K
Patient L
Patient M

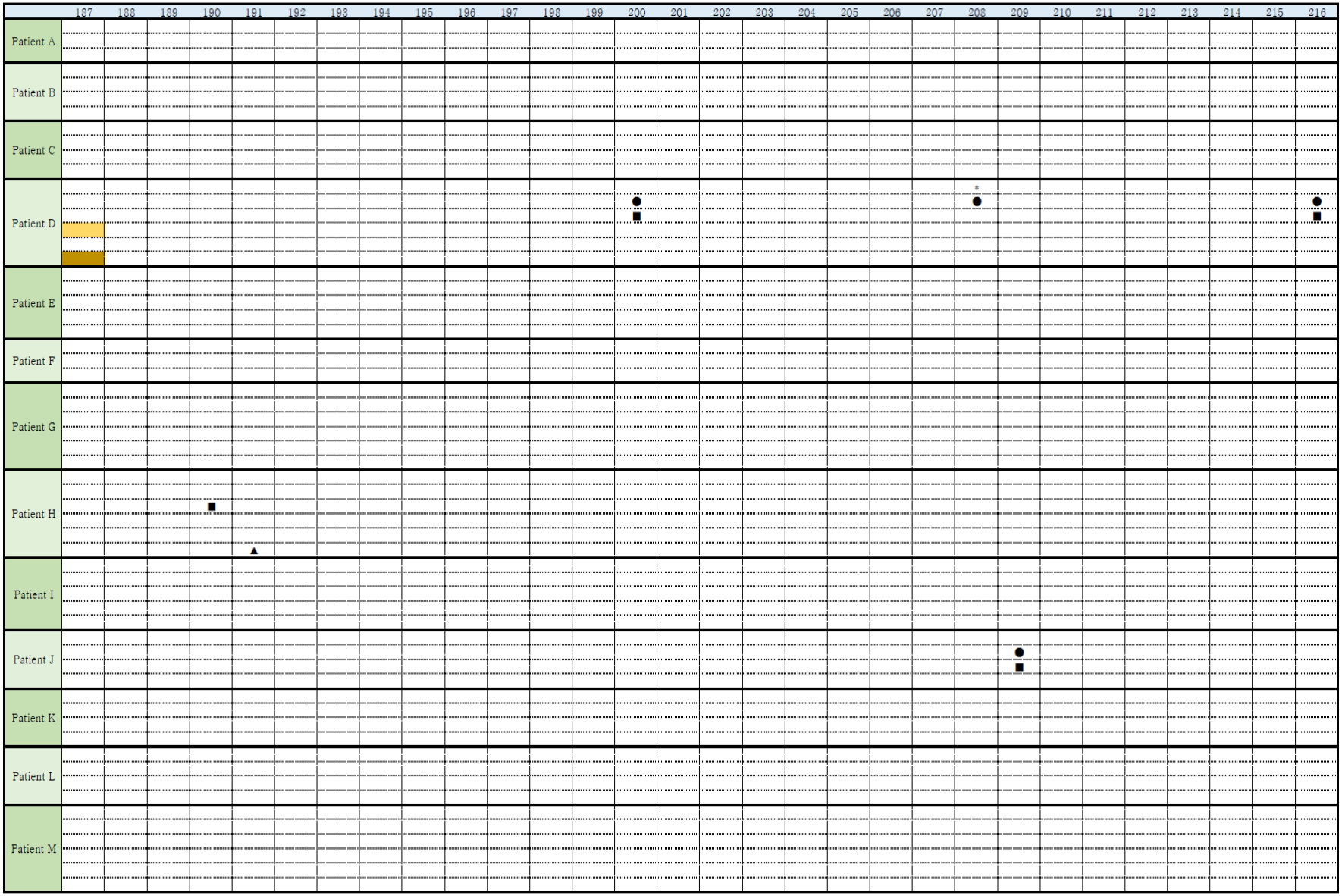
187
188
189
190
191
192
193
194
195
196
197
198
199
200
201
202
203
204
205
206
207
208
209
210
211
212
213
214
215
216
Patient A
Patient B
Patient C
Patient D
Patient E
Patient F
Patient G
Patient H
Patient I
Patient J
Patient K
Patient L
Patient M

Figure 2. The timeline for each patient, presenting when specific laboratory tests were conducted and treatments for COVID−19 were administered.

Day 0 marks the day of COVID−19 diagnosis. Asterisks denote the days when WGS was performed, while circles are used for the days with viral PCR and cultures and squares indicate the days when neutralizing antibodies were measured. Yellow boxes show the duration of remdesivir treatment for each patient, with orange and brown representing the duration of receiving dexamethasone and baricitinib, respectively. Inverted triangles mark the days when tocilizumab was administered to the patients, while regular triangles present the days when tixagevimab−cilgavimab was given.

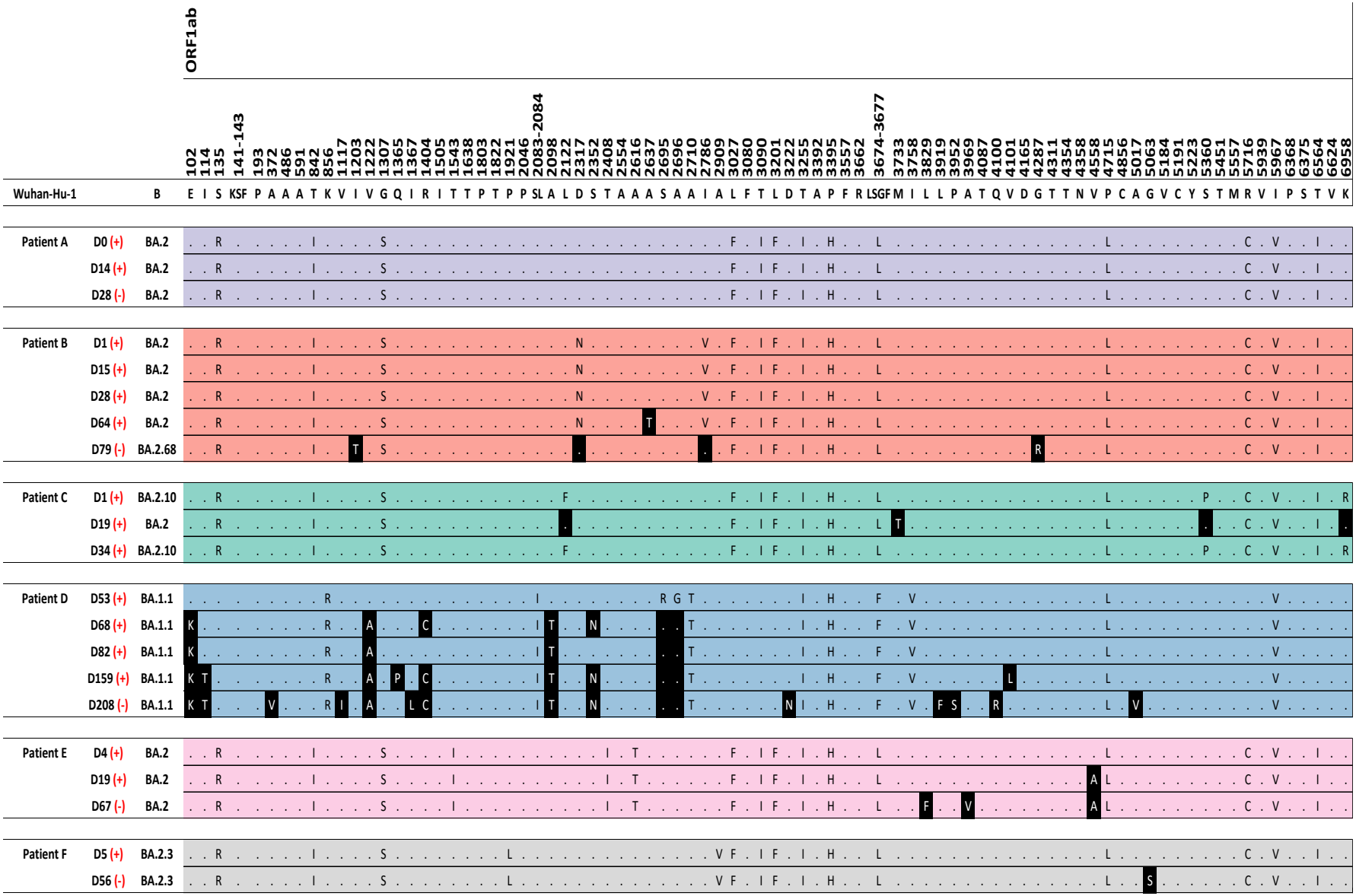
ORF1ab
102 114 135 141-143 193 372 486 591 842 856 1117 1203 1222 1307 1365 1367 1404 1505 1543 1638 1803 1822 1921 2046 2083-2084 2098 2122 2317 2352 2408 2554 2616 2637 2695 2696 2710 2786 2909 3027 3080 3090 3201 3222 3255 3392 3395 3557 3662 3674-3677 3733 3758 3829 3919 3952 3969 4087 4100 4101 4165 4287 4311 4354 4358 4558 4715 4856 5017 5063 5184 5191 5223 5360 5451 5557 5716 5939 5967 6368 6375 6564 6624 6958
Wuhan-Hu-1 B E I S KSF P A A A T K V I V G Q I R I T T P T P P SL A L D S T A A A S A A I A L F T L D T A P F R LSGF M I L L P A T Q V D G T T N V P C A G V C Y S T M R V I P S T V K
Patient A D0 (+) BA.2
D14 (+) BA.2
D28 (-) BA.2
Patient B D1 (+) BA.2
D15 (+) BA.2
D28 (+) BA.2
D64 (+) BA.2
D79 (-) BA.2.68
Patient C D1 (+) BA.2.10
D19 (+) BA.2
D34 (+) BA.2.10
Patient D D53 (+) BA.1.1
D68 (+) BA.1.1
D82 (+) BA.1.1
D159 (+) BA.1.1
D208 (-) BA.1.1
Patient E D4 (+) BA.2
D19 (+) BA.2
D67 (-) BA.2
Patient F D5 (+) BA.2.3
D56 (-) BA.2.3

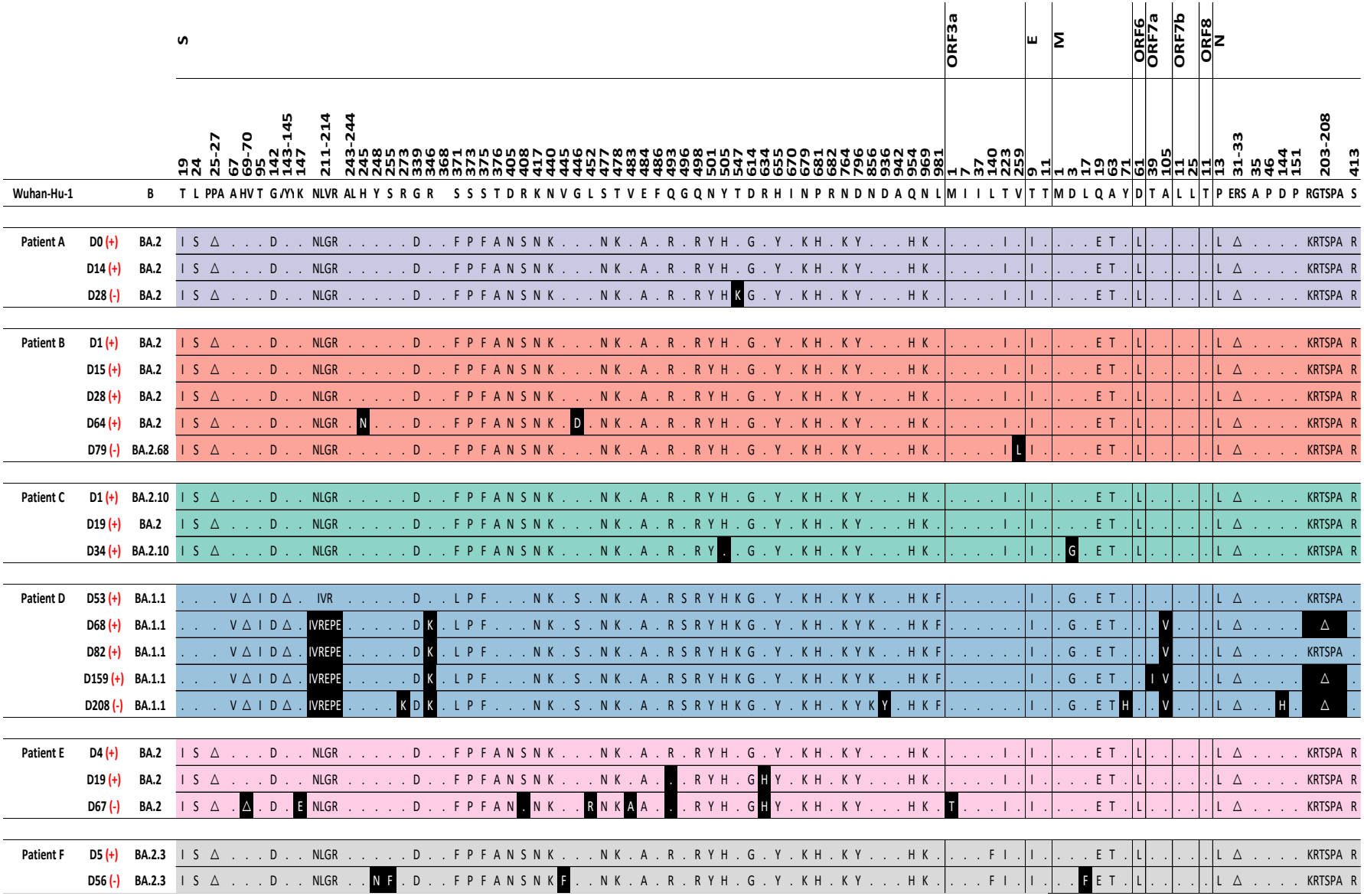
S
ORF3a
E
M
ORF6
ORF7a
ORF7b
ORF8
N
Wuhan-Hu-1 B
Patient A D0 (+) BA.2
D14 (+) BA.2
D28 (-) BA.2
Patient B D1 (+) BA.2
D15 (+) BA.2
D28 (+) BA.2
D64 (+) BA.2
D79 (-) BA.2.68
Patient C D1 (+) BA.2.10
D19 (+) BA.2
D34 (+) BA.2.10
Patient D D53 (+) BA.1.1
D68 (+) BA.1.1
D82 (+) BA.1.1
D159 (+) BA.1.1
D208 (-) BA.1.1
Patient E D4 (+) BA.2
D19 (+) BA.2
D67 (-) BA.2
Patient F D5 (+) BA.2.3
D56 (-) BA.2.3

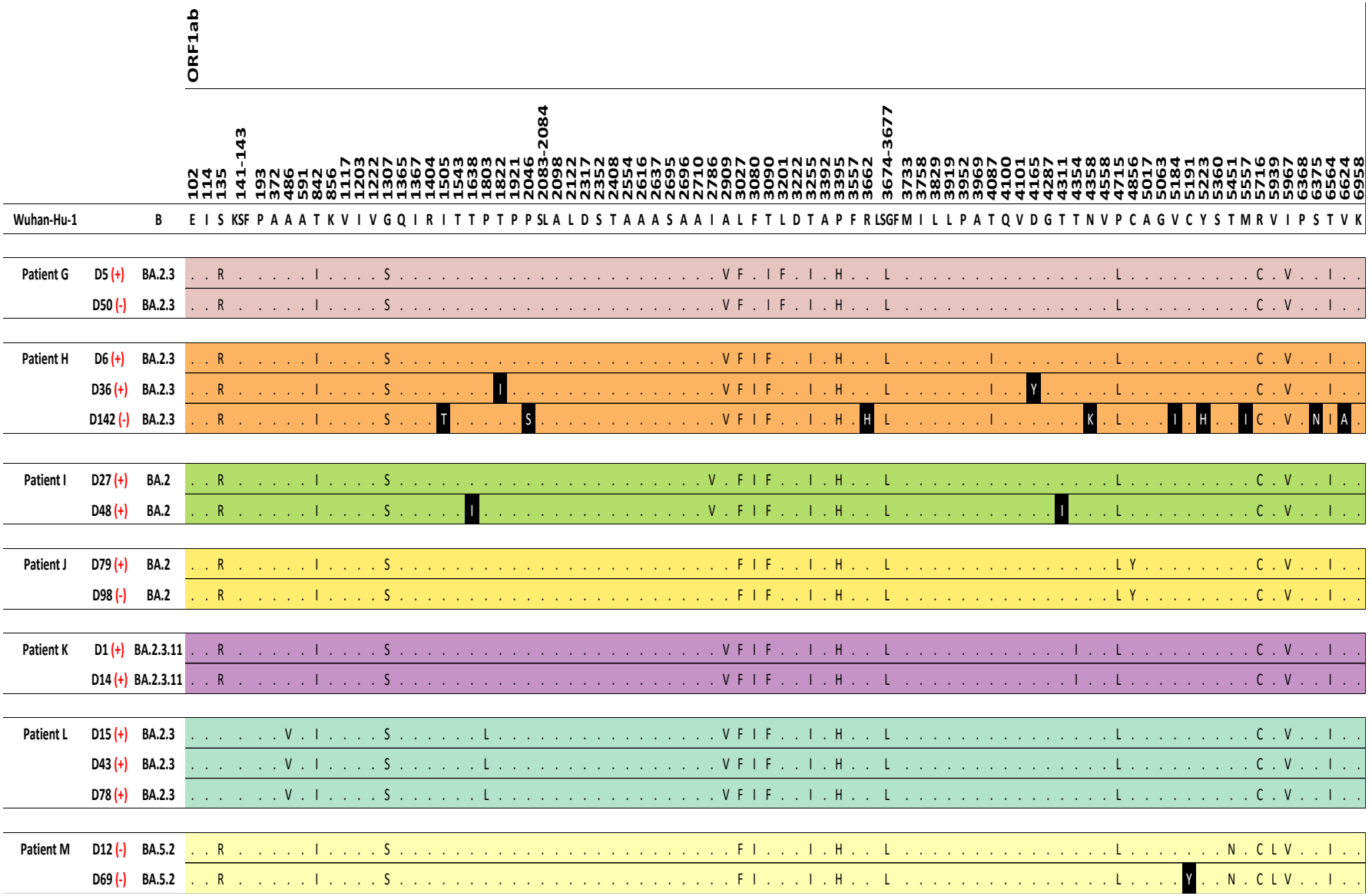
ORF1ab
102 114 135 141-143 193 372 486 591 842 856 1117 1203 1222 1307 1365 1367 1404 1505 1543 1638 1803 1822 1921 2046 2083-2084 2098 2122 2317 2352 2408 2554 2616 2637 2695 2696 2710 2786 2909 3027 3080 3090 3201 3222 3255 3392 3395 3557 3662 3674-3677 3733 3758 3829 3919 3952 3969 4087 4100 4101 4165 4287 4311 4354 4358 4558 4715 4856 5017 5063 5184 5191 5223 5360 5451 5557 5716 5939 5967 6368 6375 6564 6624 6958
Wuhan-Hu-1 B E I S KSF P A A A T K V I V G Q I R I T T P T P P SL A L D S T A A A S A A I A L F T L D T A P F R LSGF M I L L P A T Q V D G T T N V P C A G V C Y S T M R V I P S T V K
Patient G D5 (+) BA.2.3 . . R . . . . . I . . . . S . . . . . V F . I F . I . H . . L . . . . . L . . . . . C . V . . I . .
D50 (-) BA.2.3 . . R . . . . . I . . . . S . . . . . V F . I F . I . H . . L . . . . . L . . . . . C . V . . I . .
Patient H D6 (+) BA.2.3 . . R . . . . . I . . . . S . . . . . V F I F . . I . H . . L . . . . . I . . . . . L . . . . . C . V . . I . .
D36 (+) BA.2.3 . . R . . . . . I . . . . S . . . . . I . . . . . V F I F . . I . H . . L . . . . . I . . Y . . . . L . . . . . C . V . . I . .
D142 (-) BA.2.3 . . R . . . . . I . . . . S . . . T . . . . . S . . . . . V F I F . . I . H . H L . . . . . I . . . . . K . L . . . I . H . . I C . V . N I A .
Patient I D27 (+) BA.2 . . R . . . . . I . . . . S . . . . . V . F I F . . I . H . . L . . . . . L . . . . . C . V . . I . .
D48 (+) BA.2 . . R . . . . . I . . . . S . . . . . I . . . . . V . F I F . . I . H . . L . . . . . I . . . L . . . . . C . V . . I . .
Patient J D79 (+) BA.2 . . R . . . . . I . . . . S . . . . . F I F . . I . H . . L . . . . . L Y . . . . . C . V . . I . .
D98 (-) BA.2 . . R . . . . . I . . . . S . . . . . F I F . . I . H . . L . . . . . L Y . . . . . C . V . . I . .
Patient K D1 (+) BA.2.3.11 . . R . . . . . I . . . . S . . . . . V F I F . . I . H . . L . . . . . I . . L . . . . . C . V . . I . .
D14 (+) BA.2.3.11 . . R . . . . . I . . . . S . . . . . V F I F . . I . H . . L . . . . . I . . L . . . . . C . V . . I . .
Patient L D15 (+) BA.2.3 . . . . . V . I . . . . S . . . . . L . . . . . V F I F . . I . H . . L . . . . . L . . . . . C . V . . I . .
D43 (+) BA.2.3 . . . . . V . I . . . . S . . . . . L . . . . . V F I F . . I . H . . L . . . . . L . . . . . C . V . . I . .
D78 (+) BA.2.3 . . . . . V . I . . . . S . . . . . L . . . . . V F I F . . I . H . . L . . . . . L . . . . . C . V . . I . .
Patient M D12 (-) BA.5.2 . . R . . . . . I . . . . S . . . . . F I . . . I . H . . L . . . . . L . . . . . N . C L V . . I . .
D69 (-) BA.5.2 . . R . . . . . I . . . . S . . . . . F I . . . I . H . . L . . . . . L . . . . Y . . N . C L V . . I . .

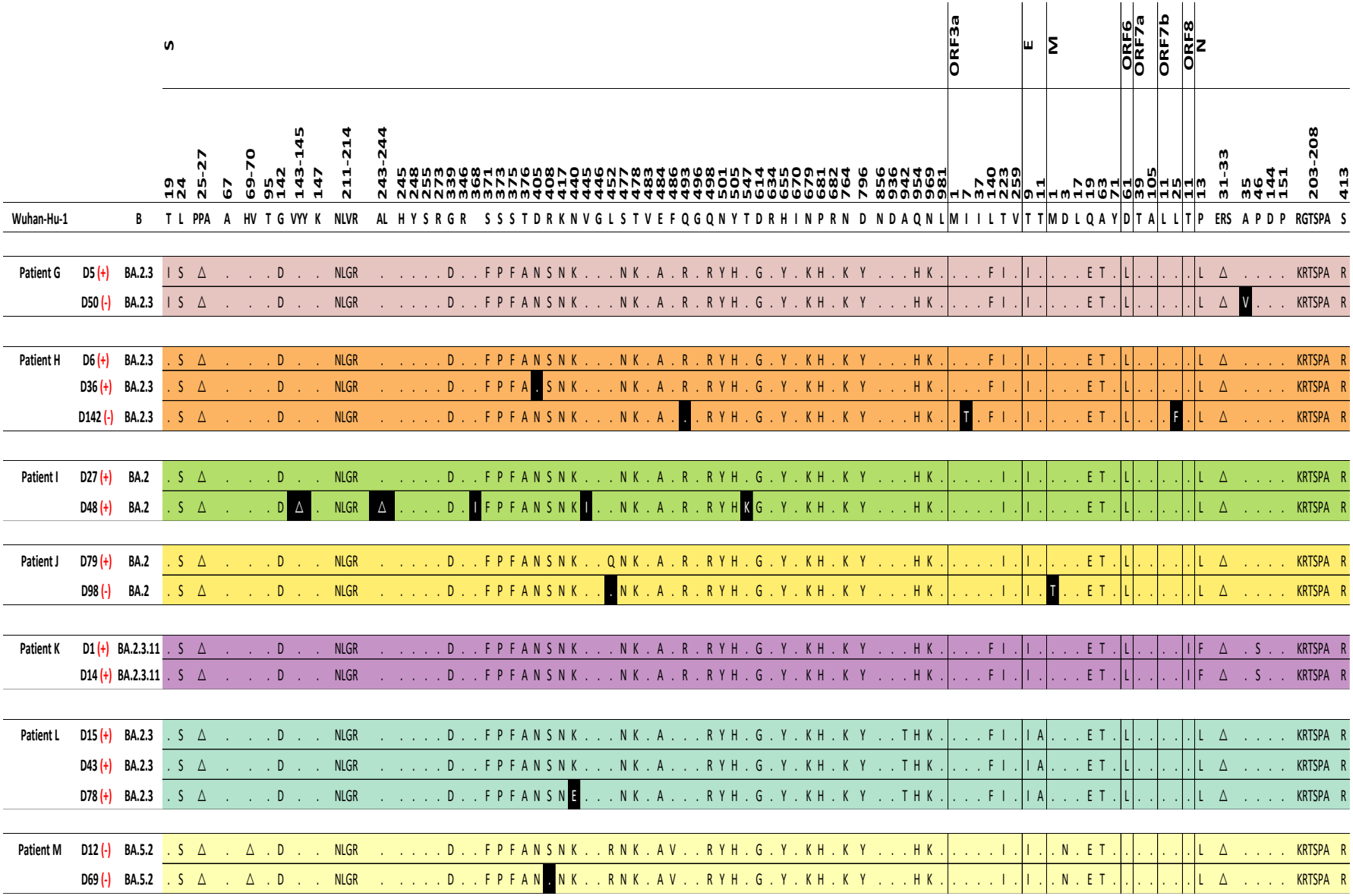
S
ORF3a
E
M
ORF6
ORF7a
ORF7b
ORF8
N
Wuhan-Hu-1 B T L PPA A HV T G VYY K NLVR AL H Y S R G R S S S T D R K N V G L S T V E F Q G Q N Y T D R H I N P R N D N D A Q N L M I I L T V T T M D L Q A Y D T A L L T P ERS A P D P RGTSPA S
Patient G D5 (+) BA.2.3 I S Δ . . . D . . NLGR . . . . . D . . F P F A N S N K . . . N K . A . R . R Y H . G . Y . K H . K Y . . . H K . . . F I . I . . . E T . L . . . . . L Δ . . . . KRTSPA R
D50 (-) BA.2.3 I S Δ . . . D . . NLGR . . . . . D . . F P F A N S N K . . . N K . A . R . R Y H . G . Y . K H . K Y . . . H K . . . F I . I . . . E T . L . . . . . L Δ V . . . KRTSPA R
Patient H D6 (+) BA.2.3 . S Δ . . . D . . NLGR . . . . . D . . F P F A N S N K . . . N K . A . R . R Y H . G . Y . K H . K Y . . . H K . . . F I . I . . . E T . L . . . . . L Δ . . . . KRTSPA R
D36 (+) BA.2.3 . S Δ . . . D . . NLGR . . . . . D . . F P F A . S N K . . . N K . A . R . R Y H . G . Y . K H . K Y . . . H K . . . F I . I . . . E T . L . . . . . L Δ . . . . KRTSPA R
D142 (-) BA.2.3 . S Δ . . . D . . NLGR . . . . . D . . F P F A N S N K . . . N K . A . . R Y H . G . Y . K H . K Y . . . H K . T . F I . I . . . E T . L . . . F . L Δ . . . . KRTSPA R
Patient I D27 (+) BA.2 . S Δ . . . D . . NLGR . . . . . D . . F P F A N S N K . . . N K . A . R . R Y H . G . Y . K H . K Y . . . H K . . . . I . I . . . E T . L . . . . . L Δ . . . . KRTSPA R
D48 (+) BA.2 . S Δ . . . D Δ . NLGR Δ . . . . D . I F P F A N S N K I . . N K . A . R . R Y H K G . Y . K H . K Y . . . H K . . . . I . I . . . E T . L . . . . . L Δ . . . . KRTSPA R
Patient J D79 (+) BA.2 . S Δ . . . D . . NLGR . . . . . D . . F P F A N S N K . . Q N K . A . R . R Y H . G . Y . K H . K Y . . . H K . . . . I . I . . . E T . L . . . . . L Δ . . . . KRTSPA R
D98 (-) BA.2 . S Δ . . . D . . NLGR . . . . . D . . F P F A N S N K . . . N K . A . R . R Y H . G . Y . K H . K Y . . . H K . . . . I . I . T . . E T . L . . . . . L Δ . . . . KRTSPA R
Patient K D1 (+) BA.2.3.11 . S Δ . . . D . . NLGR . . . . . D . . F P F A N S N K . . . N K . A . R . R Y H . G . Y . K H . K Y . . . H K . . . F I . I . . . E T . L . . . . I F Δ . S . . KRTSPA R
D14 (+) BA.2.3.11 . S Δ . . . D . . NLGR . . . . . D . . F P F A N S N K . . . N K . A . R . R Y H . G . Y . K H . K Y . . . H K . . . F I . I . . . E T . L . . . . I F Δ . S . . KRTSPA R
Patient L D15 (+) BA.2.3 . S Δ . . . D . . NLGR . . . . . D . . F P F A N S N K . . . N K . A . . . R Y H . G . Y . K H . K Y . . T H K . . . F I . I A . . . E T . L . . . . . L Δ . . . . KRTSPA R
D43 (+) BA.2.3 . S Δ . . . D . . NLGR . . . . . D . . F P F A N S N K . . . N K . A . . . R Y H . G . Y . K H . K Y . . T H K . . . F I . I A . . . E T . L . . . . . L Δ . . . . KRTSPA R
D78 (+) BA.2.3 . S Δ . . . D . . NLGR . . . . . D . . F P F A N S N E . . . N K . A . . . R Y H . G . Y . K H . K Y . . T H K . . . F I . I A . . . E T . L . . . . . L Δ . . . . KRTSPA R
Patient M D12 (-) BA.5.2 . S Δ . Δ . D . . NLGR . . . . . D . . F P F A N S N K . . R N K . A V . . R Y H . G . Y . K H . K Y . . . H K . . . . I . I . . N . E T . . . . . L Δ . . . . KRTSPA R
D69 (-) BA.5.2 . S Δ . Δ . D . . NLGR . . . . . D . . F P F A N . N K . . R N K . A V . . R Y H . G . Y . K H . K Y . . . H K . . . . I . I . . N . E T . . . . . L Δ . . . . KRTSPA R

Figure 3. Nonsynonymous mutations of SARS-CoV-2 acquired by each patient. Each alphabet character represents the nonsynonymous mutations compared with the Wuhan-Hu-1 reference genome, and black boxes present the newly acquired nonsynonymous mutations compared with the initial SARS-CoV-2 genome in each patient. The day on which each specimen was collected is indicated to the left, relative to the diagnosis day (D0). The results of the SARS-CoV-2 culture are displayed using red-colored symbols: (+) for positive and (-) for negative.

Table 3. Acquired nonsynonymous mutations in the SARS−CoV−2 genomes of immunocompromised patients

| Patient | Initial lineage | Acquired mutation | | |
|---|---|---|---|---|
| | | Persistent | Temporary | Undetermined |
| A | BA.2 | | | S:T547K (D28) |
| B | BA.2 | | ORF1ab:A2637T (D64) | ORF1ab:I1203T (D79) |
| | | | S:H245N (D64) | ORF1ab:N2317D (D79) |
| | | | S:G446D (D64) | ORF1ab:V2786I (D79) |
| | | | | ORF1ab:G4287R (D79) |
| | | | | ORF3:V259L (D79) |
| C | BA.2.10 | | ORF1ab:F2122L (D19) | M:D3G (D34) |
| | | | ORF1ab:M3733T (D19) | S:H505Y (D34) |
| | | | ORF1ab:P5360S (D19) | |
| | | | ORF1ab:R6958K (D19) | |
| D | BA.1.1 | ORF1ab:E102K (D68) | ORF1ab:Q1365P (D159) | ORF1ab:A372V (D208) |
| | | ORF1ab:I114T (D159) | ORF1ab:V4101L (D159) | ORF1ab:V1117I (D208) |
| | | ORF1ab:V1222A (D68) | ORF7:T39I (D159) | ORF1ab:I1367L (D208) |
| | | ORF1ab:R1404C (D159) | | ORF1ab:D3222N (D208) |
| | | ORF1ab:A2098T (D68) | | ORF1ab:L3919F (D208) |
| | | ORF1ab:S2352N (D159) | | ORF1ab:P3952S (D208) |
| | | ORF1ab:R2695S (D68) | | ORF1ab:Q4100R (D208) |

| | | | |
|---|---|---|---|
| | | ORF1ab:G2696A (D68) | ORF1ab:A5017V (D208) |
| | | S:I210V (D68) | S:R273K (D208) |
| | | S:V213E (D68) | S:D936Y (D208) |
| | | S:R346K (D68) | M:Y71H (D208) |
| | | ORF7:A105V (D68) | N:D144H (D208) |
| | | N:KRTSPA203-208Del (D159) | |
| E | BA.2 | ORF1ab:V4558A (D19) | ORF1ab:L3829F (D67) |
| | | S:R493Q (D19) | ORF1ab:A3969V (D67) |
| | | S:R634H (D19) | S:HV69-70Del (D67) |
| | | | S:K147E (D67) |
| | | | S:S408R (D67) |
| | | | S:L452R (D67) |
| | | | S:V483A (D67) |
| | | | ORF3:M1T (D67) |
| F | BA.2.3 | | ORF1ab:G5063S (D56) |
| | | | S:Y428N (D56) |
| | | | S:S255F (D56) |
| | | | S:V445F (D56) |
| | | | M:L17F (D56) |
| G | BA.2.3 | | N:A35V (D50) |

| | | | |
|---|---|---|---|
| H | BA.2.3 | ORF1ab:T1822I (D36) | ORF1ab:I1505T (D142) |
| | | ORF1ab:D4165Y (D36) | ORF1ab:P2046S (D142) |
| | | S:N405D (D36) | ORF1ab:R3662H (D142) |
| | | | ORF1ab:N4358K (D142) |
| | | | ORF1ab:V5184I (D142) |
| | | | ORF1ab:Y5223H (D142) |
| | | | ORF1ab:M5557I (D142) |
| | | | ORF1ab:S6375N (D142) |
| | | | ORF1ab:V6624A (D142) |
| | | | S:R493Q (D142) |
| | | | ORF3:I7T (D142) |
| | | | ORF7b:L25F (D142) |
| I | BA.2 | | ORF1ab:T1638I (D48) |
| | | | ORF1ab:T4311I (D48) |
| | | | S:Y144Del (D48) |
| | | | S:AL243−244Del (D48) |
| | | | S:L368I (D48) |
| | | | S:V445I (D48) |
| | | | S:T547K (D48) |
| J | BA.2 | | S:Q452L (D98) |

| | | |
|---|---|---|
| | | M:M1T (D98) |
| K | BA.2.3.11 | |
| L | BA.2.3 | S:K440E (D78) |
| M | BA.5.2 | ORF1ab:C5191Y (D69)<br>S:S408R (D69) |

Abbreviation: D, day

Each mutation is displayed alongside the day it was first detected in the respiratory specimen, relative to the diagnosis day (D0). Mutations highlighted in the underlined bold text represent those reported to be associated with immune evasion or other SARS-CoV-2 major variants.

Table 4. Characteristics of acquired nonsynonymous SARS-CoV-2 mutations in immunocompromised patients

| Patient | Immunocompromised condition | Number of acquired mutations (duration of observation) | Mutations in S region, n (%) | Mutations associated with immune evasion, n (%) | Mutations found in major variants, n (%) |
|---|---|---|---|---|---|
| A | lymphoma | 1 (28 days) | 1 (100.0) | 0 (0.0) | 1 (100.0) |
| B | AML | 8 (78 days) | 2 (25.0) | 1 (12.5) | 0 (0.0) |
| C | Kidney transplantation | 6 (33 days) | 1 (16.7) | 1 (16.7) | 2 (33.3) |
| D | Lymphoma | 28 (155 days) | 5 (17.9) | 0 (0.0) | 2 (7.1) |
| E | Lung transplantation | 11 (63 days) | 7 (63.6) | 5 (45.5) | 4 (36.4) |
| F | lymphoma | 5 (51 days) | 3 (60.0) | 1 (20.0) | 0 (0.0) |
| G | ALL | 1 (45 days) | 0 (0.0) | 0 (0.0) | 0 (0.0) |
| H | lymphoma | 15 (136 days) | 2 (13.3) | 1 (6.7) | 1 (6.7) |
| I | AML | 7 (21 days) | 5 (71.4) | 2 (28.6) | 3 (42.9) |
| J | AML | 2 (19 days) | 1 (50.0) | 1 (50.0) | 1 (50.0) |
| K | Lymphoma | 0 (13 days) | – | – | – |
| L | Lymphoma | 1 (63 days) | 1 (100.0) | 0 (0.0) | 0 (0.0) |
| M | AML | 2 (57 days) | 1 (50.0) | 0 (0.0) | 0 (0.0) |

Abbreviations: n, number; AML, acute myelogenous leukemia; ALL, acute lymphocytic leukemia

Of the 87 nonsynonymous mutations, 16 (18.4%) and 13 mutations (14.6%) were classified as persistent and temporary mutations, respectively. More than half of the mutations were detected in the ORF1ab region (Figure 4). There were 28 mutations in the S region, 12 of which were associated with immune evasion: temporary substitutions such as S:G446D and S:N405D [24,29,45] and undetermined mutations including S:K147E, S:S408R, S:L452R, S:V483A, S:V445F, S:HV69−70Del, S:Y144Del, S:AL243−244Del, S:H505Y, and S:Q452L [22,25,28,29,31,46–50]. Also, 13 mutations in the ORF1ab, S, and M regions, which included persistent substitutions such as S:I210V, S:V213E, and S:R493Q and undetermined mutations such as S:T547K, M:D3G, ORF1ab:L3829F, S:HV69−70Del, S:K147E, S:L452R, S:Y144Del, S:L368I, S:H505Y, and S:L452Q, were the defining mutations of the major variants including Omicron BA.1, BA.4, BA.5, BA.2.75, XBB, and XBB.1.5, according to the resources in CoVariant.org [3] (Table 5). Eleven of these mutations occurred in the S region. The proportion of acquired mutations that were defining mutations of the other variants was higher in the S region (11/28, 39.3%) than in the whole genomic region (13/87, 14.9%).

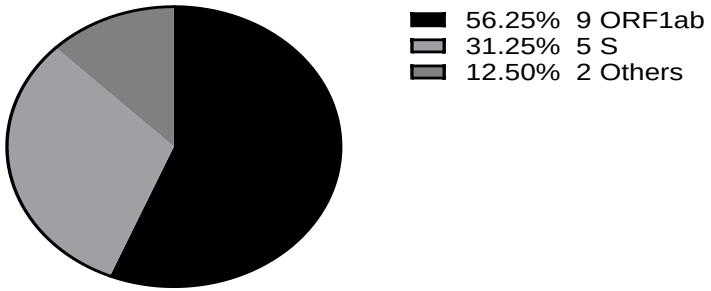


**Persistent mutations, n=16**

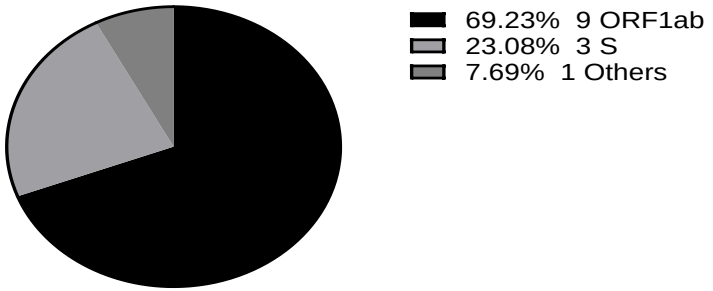


**Temporary mutations, n=13**

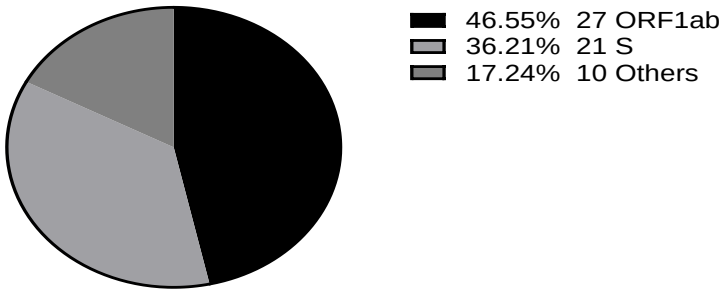


**Undetermined mutations, n=58**

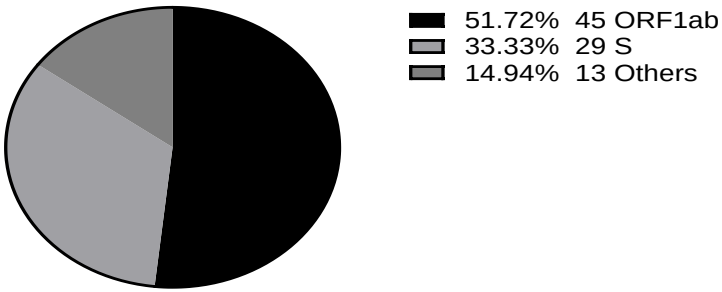


**Total mutations, n=87**

Figure 4. Distribution of nonsynonymous mutations in each region of SARS-CoV-2 genomes

Abbreviations: n, number; ORF, open reading frame; S, spike

Table 5. Acquired nonsynonymous mutations that are defining mutations of other major variants

| Nonsynonymous mutation | Associated major variants |
|---|---|
| ORF1ab:L3829F | BQ.1, XBB.1.16 |
| S:HV69−70Del | B.1.1.7 (Alpha), B.1.525 (Eta), BA.1, BA.4, BA.5, BQ.1 |
| S:Y144Del | B.1.1.7 (Alpha), B.1.525 (Eta), BA.1, XBB, XBB.1.5, XBB.1.16 |
| S:K147E | BA.2.75 |
| S:I210V | BA.2.75 |
| S:V213E | XBB, XBB.1.5, XBB.1.16 |
| S:L368I | XBB, XBB.1.5, XBB.1.16 |
| S:L452Q | BA.2.12.1, C.37 (Lambda) |
| S:L452R | BA.4, BA.5, BQ.1, B.1.617.1 (Kappa), B.1.427/B.1.429 (Epsilon), B.1.617.2 (Delta) |
| S:R493Q | BA.2.75, BQ.1, XBB, XBB.1.5, XBB.1.16 |
| S:Y505H | BA.4, BA.5, BA.2.12.1, BA.2.75, BQ.1, XBB, XBB.1.5, XBB.1.16 |
| S:T547K | BA.1 |
| M:D3G | BA.1 |

## 3. Rates of acquisition of nonsynonymous mutations

Nonsynonymous mutations in the SARS-CoV-2 genome were acquired at a different rate in each patient (Figure 5). In particular, patient D acquired more mutations in an especially short time. This patient was immunocompromised as a result of treatment with rituximab and epocoritamab for lymphoma less than six months before the diagnosis of COVID-19 infection. Despite receiving three doses of the SARS-CoV-2 vaccine, the patient's blood samples contained insufficient neutralizing antibodies against the Omicron variant. This patient underwent a longer course of COVID-19 treatment, which included remdesivir, steroids, and baricitinib, compared to others. Similarly, patients E and H acquired more mutations within the same period than other patients. These two patients also had low titers of neutralizing antibodies and received COVID-19 treatment with remdesivir, steroids, or baricitinib for over two weeks (Table 6).

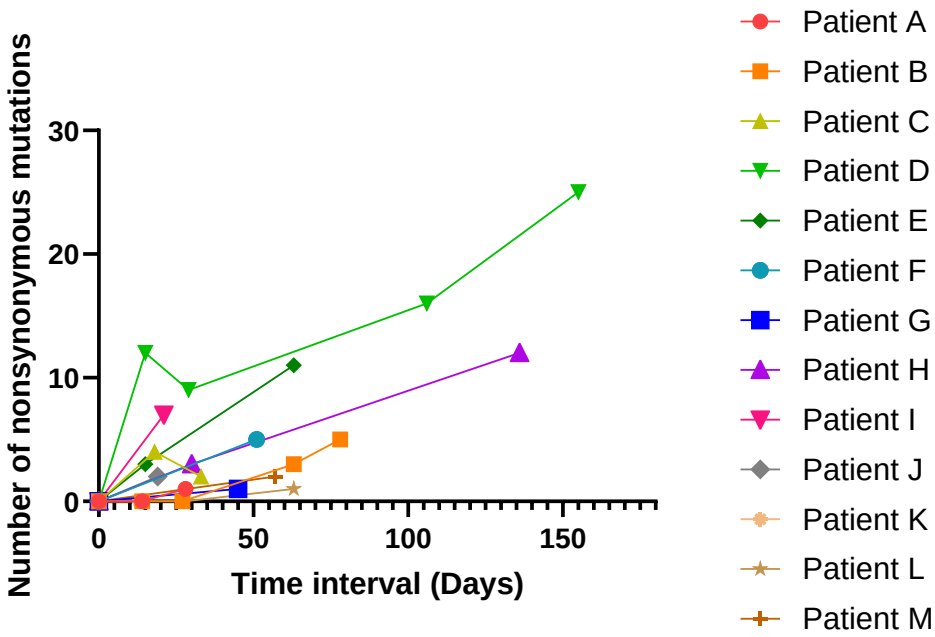


Figure 5. The number of the nonsynonymous mutations in sequenced SARS-CoV-2 genomes in each patient over time

The first day when WGS analysis was performed for each patient was considered day 0.

Table 6. Histories of other treatments and durations of COVID-19 treatments in the immunocompromised patients

| Patient | Immunocompromised condition | Treatment history | SARS-CoV-2 vaccination | Median of neutralizing Ab (ND50) | Duration of culture positivity (days) | Total number of acquired mutations (duration of observation) | Duration of COVID-19 treatments (days) | | | | |
|---|---|---|---|---|---|---|---|---|---|---|---|
| | | | | | | | RDV | DXM | Other steroid[a] | TCZ | BCT |
| A | Lymphoma | - | Partial | - | 28 | 1 (28 days) | 3 | 0 | 0 | 0 | 0 |
| B | AML, HSCT | - | None | 802.8 | 75 | 8 (78 days) | 5 | 0 | 0 | 0 | 0 |
| C | Kidney transplant | Tacrolimus, prednisolone, rituximab | Full | 182.7 | 55 | 6 (33 days) | 3 | 0 | 0 | 0 | 0 |
| D | Lymphoma | Rituximab, epocoritamab | Full | 8.1 | 155 | 28 (155 days) | 29 | 16 | 103 | 1 | 35 |
| E | Lung transplant | Tacrolimus, mycophenolate mofetil | None | 181.2 | 55 | 11 (63 days) | 17 | 11 | 51 | 0 | 0 |
| F | Lymphoma | Rituximab | None | - | 56 | 5 (51 days) | 3 | 0 | 0 | 0 | 0 |

| | | | | | | | | | | | |
|---|---|---|---|---|---|---|---|---|---|---|---|
| G | ALL, HSCT | – | Partial | 463.4 | 50 | 1 (45 days) | 6 | 10 | 0 | 1 | 0 |
| H | Lymphoma, HSCT | Rituximab | None | 14.1 | 58 | 15 (136 days) | 28 | 17 | 72 | 0 | 15 |
| I | AML, HSCT | – | None | 693.3 | 55 | 7 (21 days) | 5 | 6 | 0 | 0 | 0 |
| J | AML, HSCT | – | None | 1563.5 | 84 | 2 (19 days) | 11 | 0 | 0 | 0 | 0 |
| K | Lymphoma | Rituximab | Partial | 228.2 | 50 | 0 (13 days) | 3 | 0 | 0 | 0 | 0 |
| L | Lymphoma | Rituximab | None | 64.6 | 78 | 1 (63 days) | 5 | 0 | 0 | 0 | 0 |
| M | AML, HSCT | – | None | 164.3 | 36 | 2 (57 days) | 10 | 9 | 0 | 1 | 15 |

Abbreviations: SARS-CoV-2, Severe Acute Respiratory Syndrome-Coronavirus-2; Ab, antibodies; ND50, 50% neutralization dose; COVID-19, Coronavirus disease-19; RDV, remdesivir; DXM, dexamethasone; TCZ, tocilizumab; BCT, baricitinib; AML, acute myelogenous leukemia; HSCT, hematopoietic stem cell transplantation; ALL, acute lymphocytic leukemia

[a] High-dose steroids more than equivalent doses of prednisolone 0.3 mg/kg/day

## 4. Nonsynonymous mutations associated with remdesivir resistance

SARS-CoV-2 RNA-dependent RNA polymerase (RdRp) is located in the ORF1ab region and encoded by *nsp12*, which interacts with essential cofactors *nsp7* and *nsp8* to form the RdRp complex [11,51]. V792I in the *nsp12* (V5184I of the ORF1ab region) is reported to be associated with decreased viral sensitivity to remdesivir [10,11], and patient H acquired this mutation 142 days after diagnosis of SARS-CoV-2 infection. Before the acquisition of this mutation, the patient had been exposed to five cycles of remdesivir, three cycles of dexamethasone, and one cycle of baricitinib for 28, 17, and 15 days, respectively (Figure 6). This patient also received high-dose steroids (≥ equivalent doses of prednisolone 0.3 mg/kg daily) for more than two months (not shown in the graph of Figure 4). Patients D and E also received more than two cycles of remdesivir and maintained high-dose steroids for about two months, similar to patient H. However, unlike patient H, they did not acquire any mutation associated with resistance to remdesivir (Table 6).

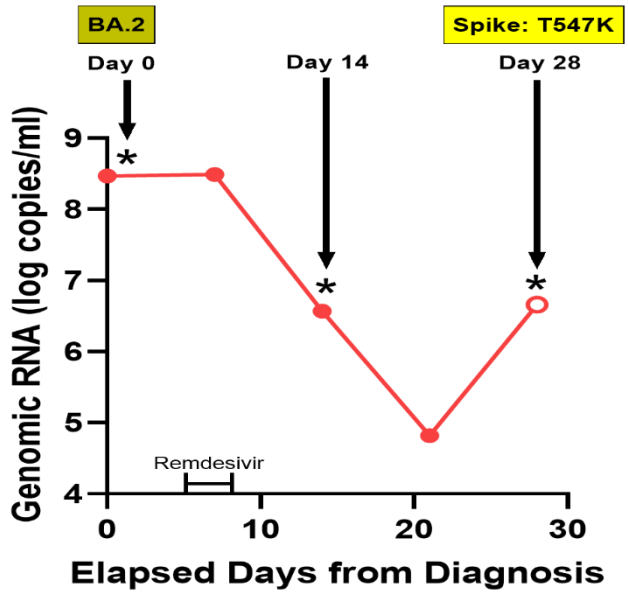


Patient A

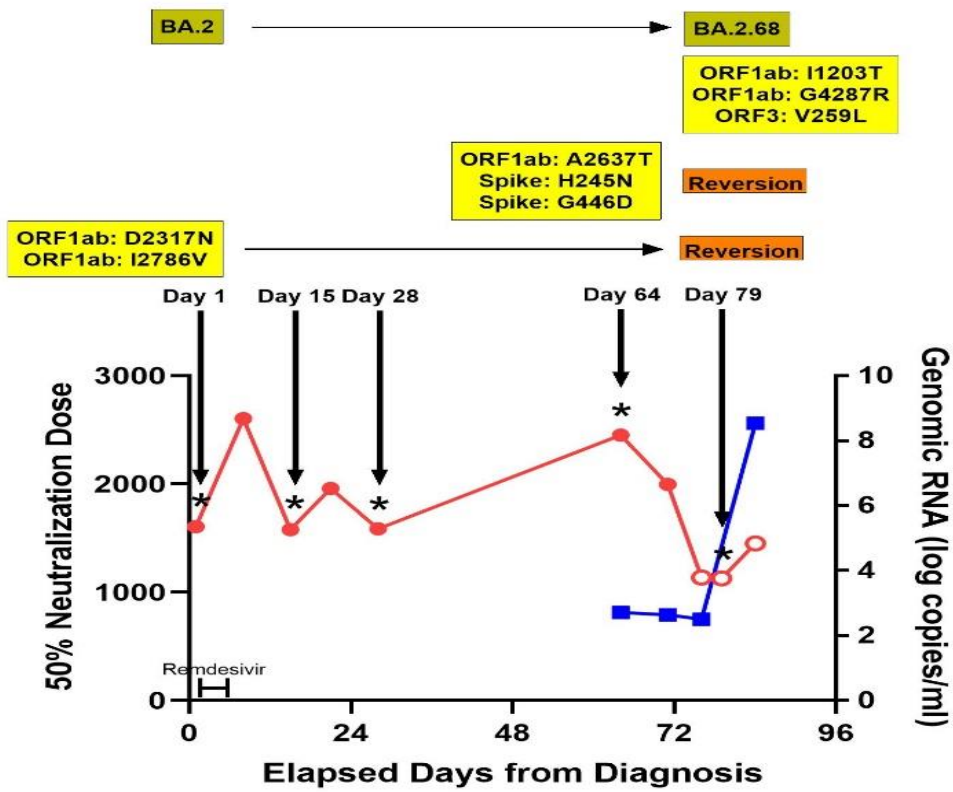


Patient B

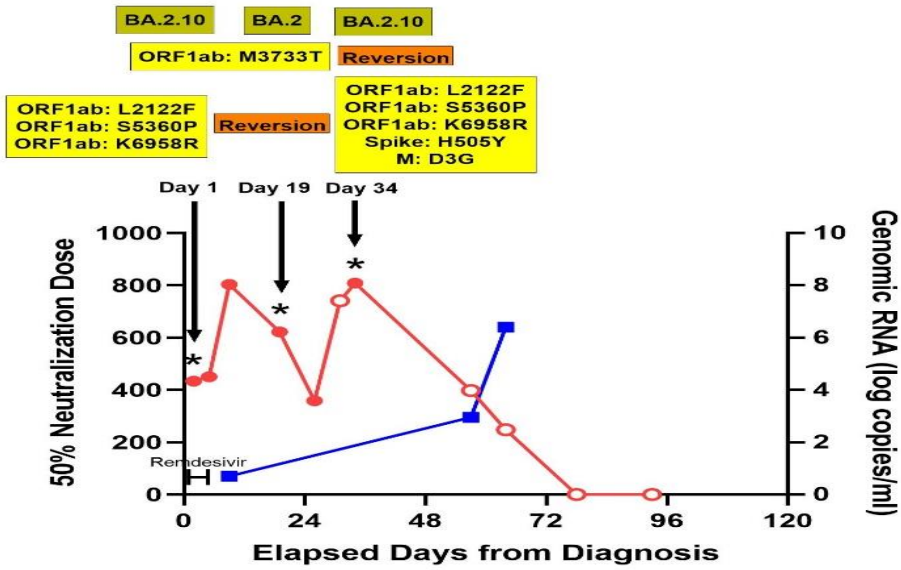


**Patient C**

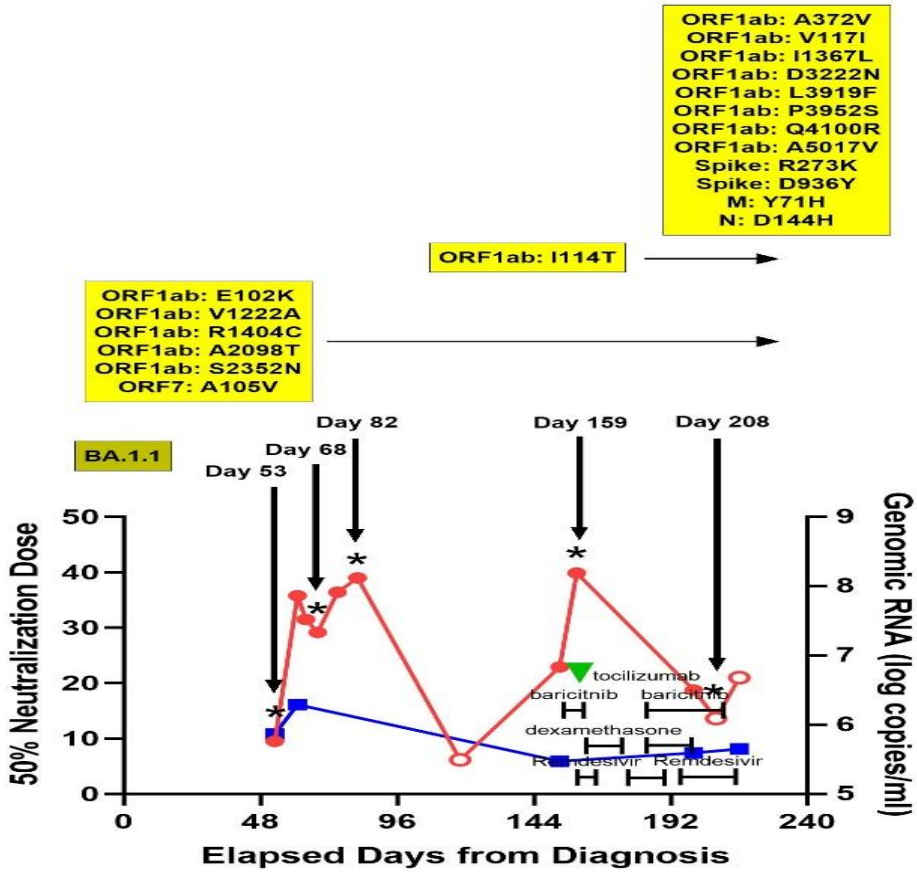


**Patient D**

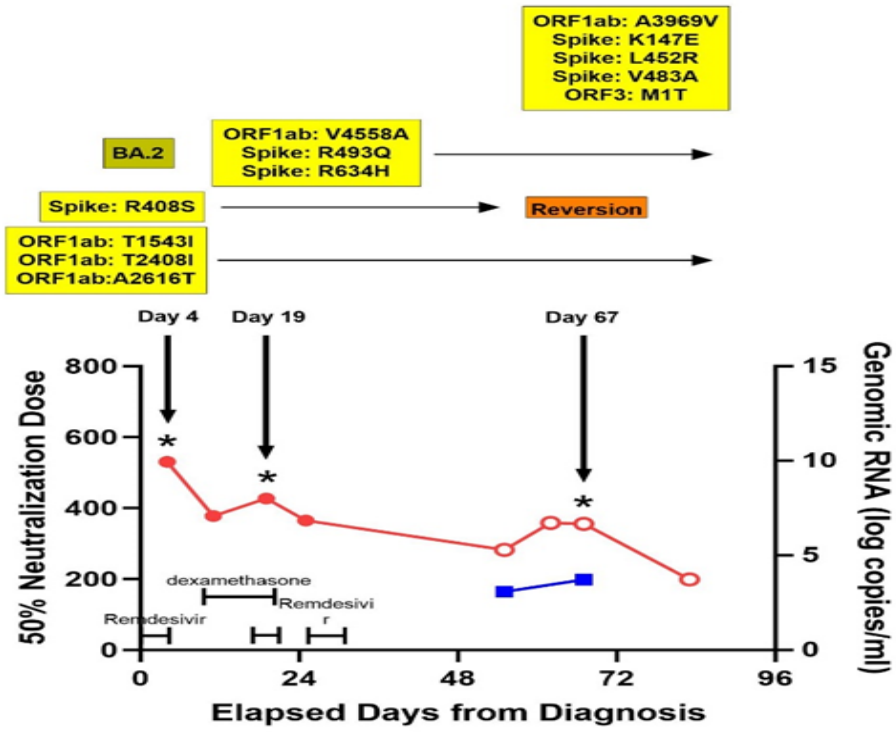


Patient E

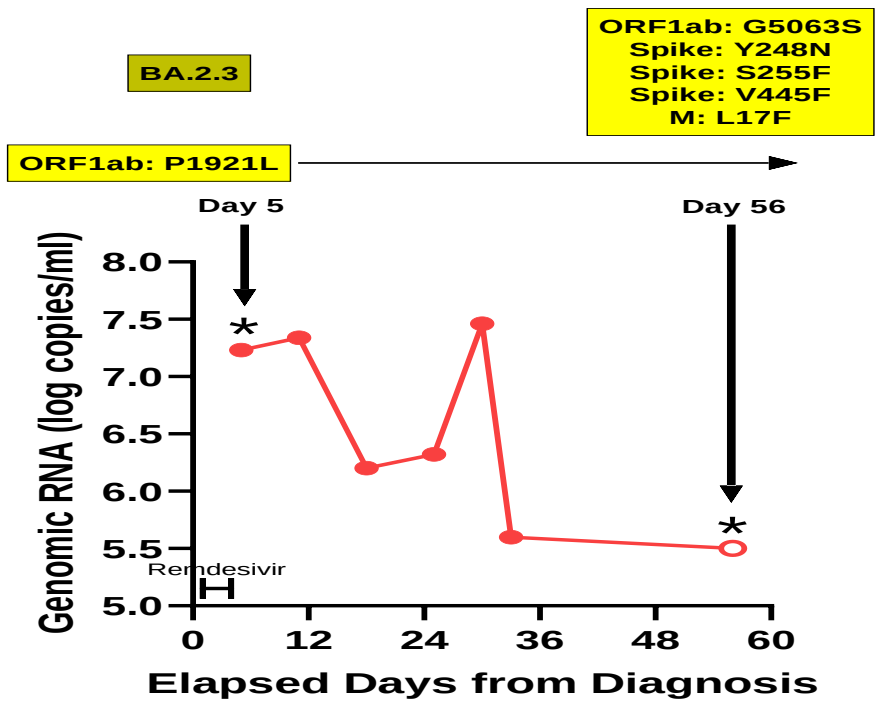


Patient F

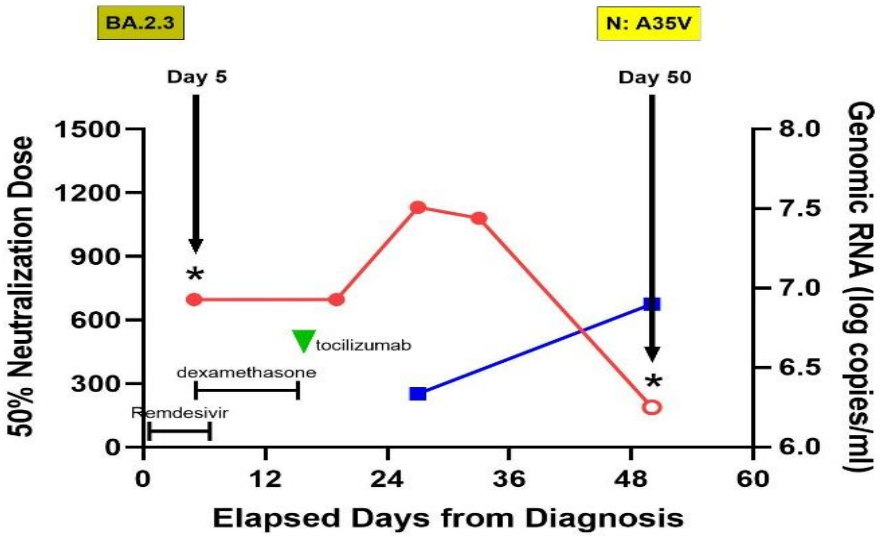


**Patient G**

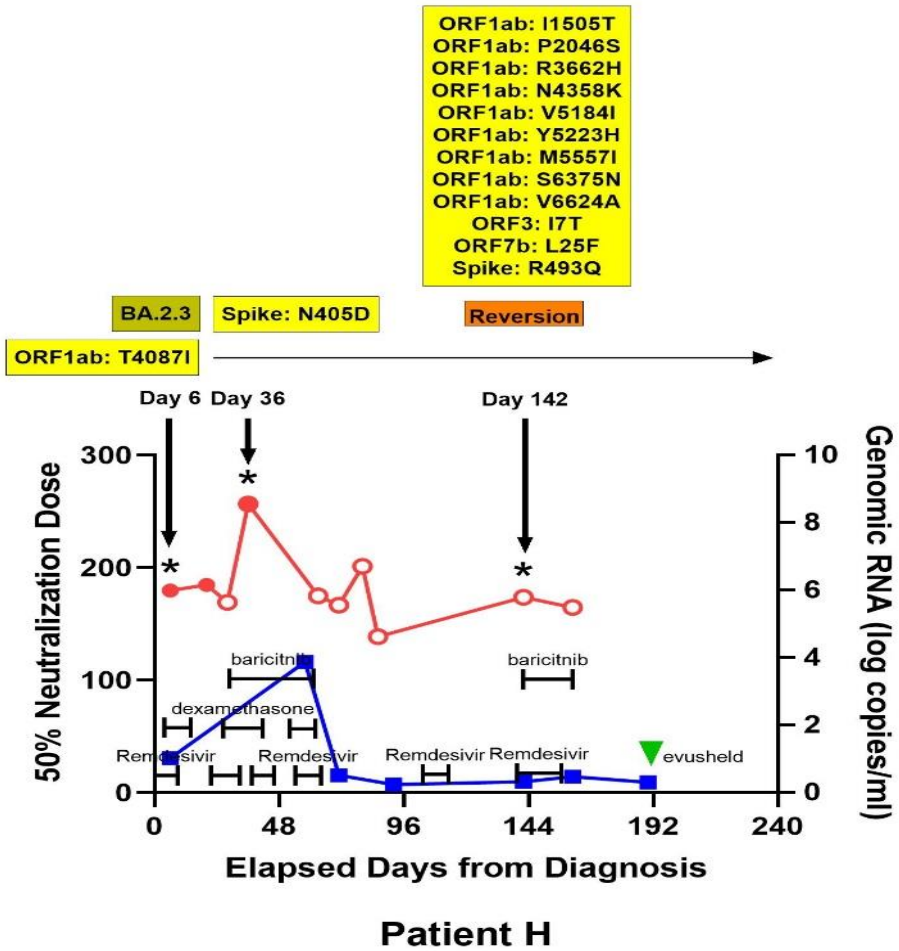


**Patient H**

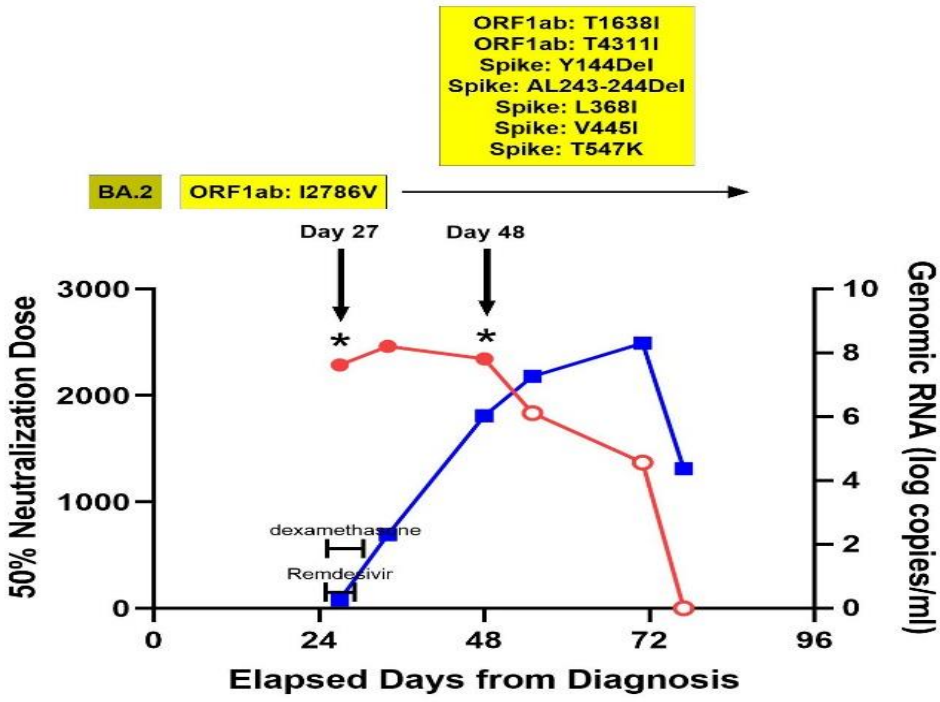


Patient I

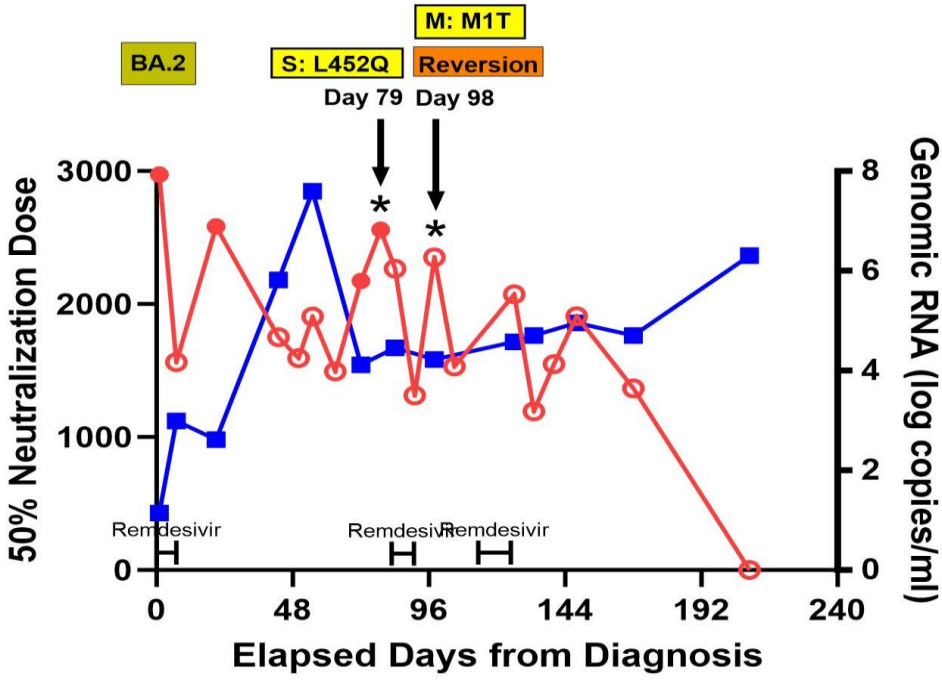


Patient J

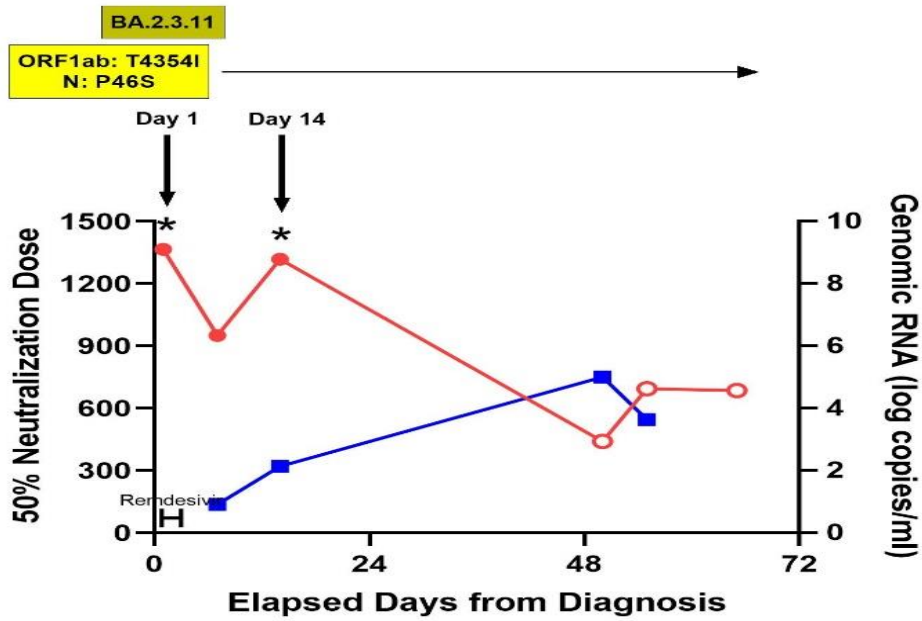


Patient K

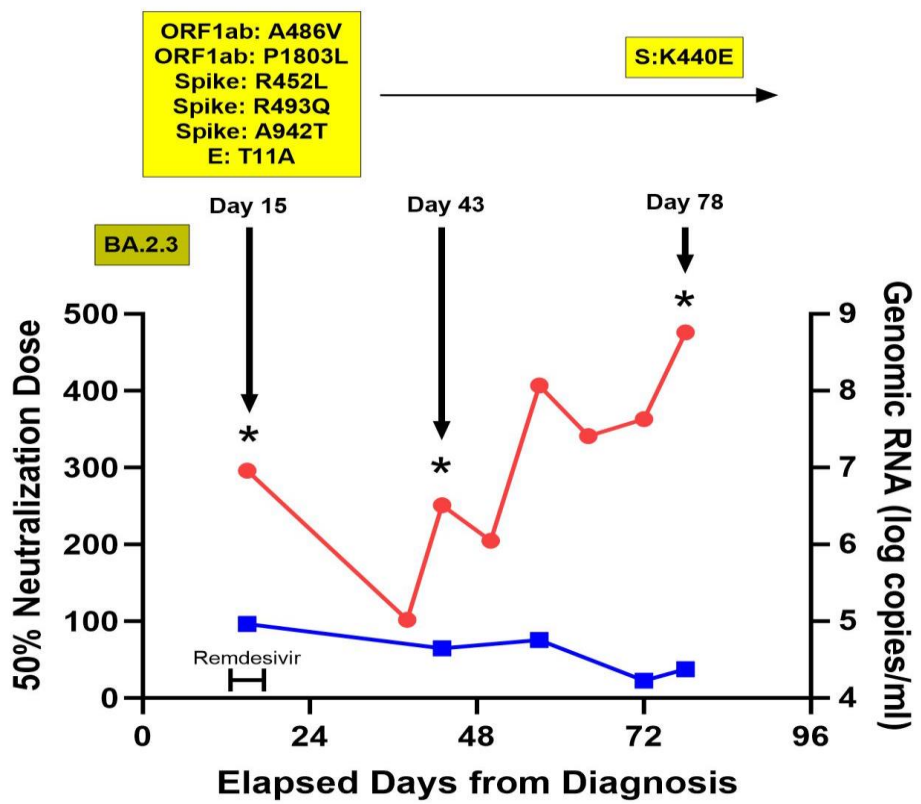


Patient L

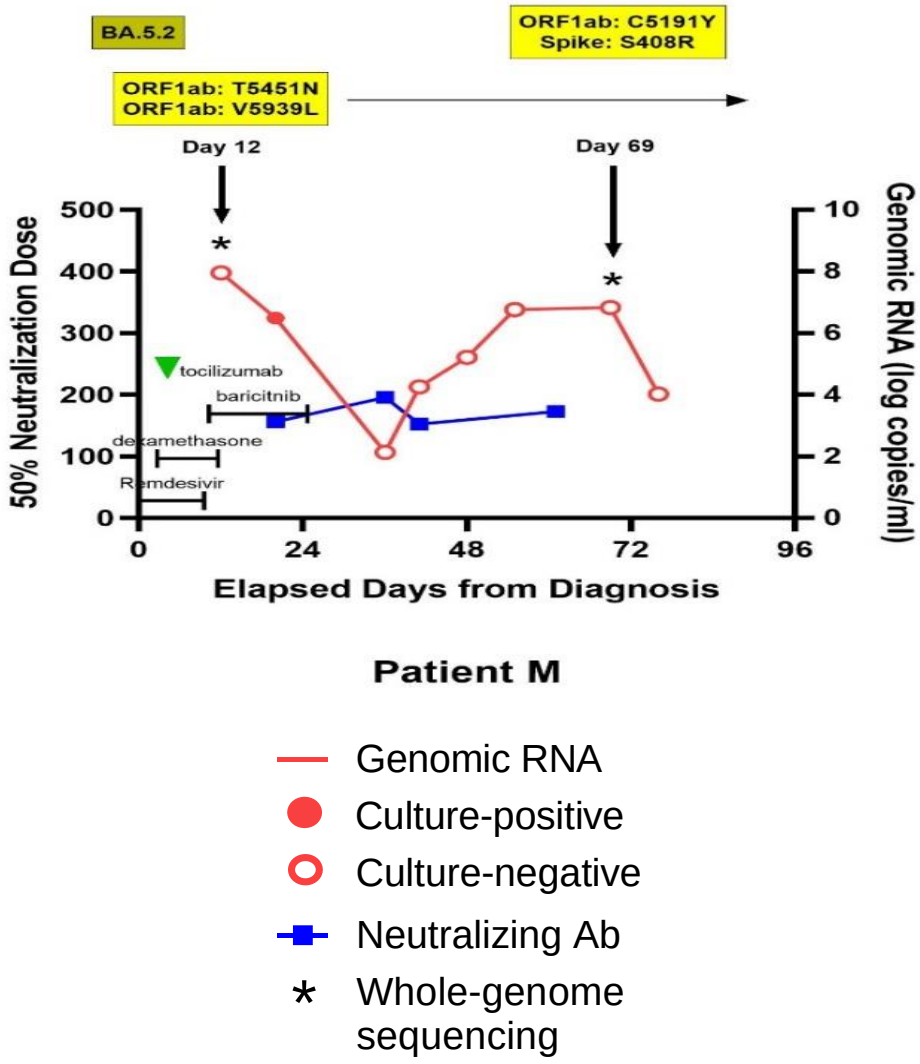


Figure 6. Changes of SARS-CoV-2 viral loads, titers of neutralizing antibodies, and nonsynonymous mutations in sequenced SARS-CoV-2 genomes in each patient over time and COVID-19 treatments used

## 5. Persistent viral shedding in spite of high titers of neutralizing antibodies

The titer of neutralizing antibodies against the Omicron subvariant that they were infected with was measured using serum samples from 11 patients. Figure 6 shows changes in SARS-CoV-2 viral load and titers of neutralizing antibodies over time after diagnosis of SARS-CoV-2 infection, culture positivity at each point, the times when WGS analyses were conducted, and duration of COVID-19 treatment for each patient. In most patients, negative conversion of the viral culture occurred when the titer of neutralizing antibodies started to rise steeply and maintained a high level (Figure 6). However, despite maintaining a high titer of neutralizing antibodies from the time of diagnosis of COVID-19 infection, patient J shed the virus persistently from day 72 to day 79. In patient J, WGS analyses were conducted on day 79 and day 98. The missense mutation S:L452Q, observed on day 79, had "reverted" by day 98. This mutation has been reported to be associated with immune evasion and a decreased sensitivity to neutralizing antibodies [25,31]. It's unclear when the mutation emerged and disappeared, but its presence might have been linked to persistent viral shedding from day 72 to day 79, despite the presence of a high titer of neutralizing antibodies.

# Chapter IV. Discussion

This study described the characteristics and dynamics of acquired mutations in the SARS-CoV-2 genome of immunocompromised individuals with persistent viral detection. Our research has several advantages over previous studies. Firstly, our analyses included a larger number of immunocompromised patients. Secondly, we conducted mutational analyses during the Omicron-prevalent period to identify the emergence of mutations defining other Omicron subvariants. Finally, we concurrently measured neutralizing antibodies to better understand how their titers impact viral shedding.

We observed that each patient acquired a median of two amino acid substitutions, excluding temporary mutations, over an observation period of 51 days, which equals 14.2 substitutions per year. In comparison, other studies have reported rates of nonsynonymous mutation acquisition, again excluding temporary mutations, in immunocompromised individuals, ranging from 24.4 to 52.4 substitutions over a year [7,19,21]. Our study included a larger number of immunocompromised patients than previous studies. Some patients in our study had a lesser degree of immunocompromise

compared to those in previous studies, which could lead to variations in the mutation acquisition rates among the studies.

Patients D, E, and H were significantly immunocompromised due to underlying conditions and extended steroid therapy. Consequently, they acquired mutations in the SARS-CoV-2 genome more rapidly than other patients in this study. Their rates of nonsynonymous mutation acquisition ranged from 39.7 to 62.9 per year. These rates exceed the estimated average rates of evolution for both SARS-CoV-2, which is about 26.6 substitutions per year, and influenza A (H1N1), which ranges from 8.4 to $28.0\times10^{-3}$ mutations per year [52–55]. Moreover, an immunocompromised patient with influenza A (H1N1) displayed nonsynonymous mutations in the hemagglutinin gene at a rate of 5.6-16.2 per year. This rate is slower than the mutation rates calculated for SARS-CoV-2 in these highly immunosuppressed individuals [56]. Therefore, some severely immunocompromised patients with SARS-CoV-2 could accumulate a significantly larger number of mutations in the SARS-CoV-2 genome compared to the general population or individuals with influenza. This could potentially indicate that various VOCs or VOIs of SARS-CoV-2 have emerged more rapidly over the last three years compared to the cases of influenza.

As described above in patients D, E, and H, there might be

a tendency for more rapid development of mutations in immunocompromised individuals who take remdesivir or high-dose steroids for extended periods. The prolonged administration of steroids could impair cellular immunity, delay clearance of SARS-CoV-2, and lead to the accumulation of mutations in the viral genome [15,16,57]. In addition, the extended use of remdesivir might hasten the "fixation" of acquired mutations and the advent of new variants [58]. Furthermore, patients with B-cell depletion could be more susceptible to the development of new SARS-CoV-2 variants and remdesivir resistance with the prolonged use of remdesivir [58]. The potential association between prolonged administration of remdesivir or steroids and increased acquisition of mutations in the SARS-CoV-2 genome could be examined in further studies involving more immunocompromised patients.

Several mutations seem to have emerged sporadically, distributed throughout the entire SARS-CoV-2 genome. This distribution pattern mirrors findings from earlier studies that also reported a sporadic distribution of various mutations across the SARS-CoV-2 genome in immunocompromised patients [12,13]. The ORF1ab region, accounting for up to 21,290 nucleotides (71.2%) of the 29,900 total and representing the longest genomic region of SARS-CoV-2 [59], harbored more than half of the nonsynonymous

mutations identified in the immunocompromised patients of this study. The S region, consisting of 3,822 nucleotides (12.8%) [60], harbored about one-third of the nonsynonymous mutations. The adjusted mutation numbers per kilobase were 2.1 for the ORF1ab region and 7.6 for the S region. A previous study also showed a higher mutation rate in the S region than in the ORF1ab region [61]. Additionally, mutations known to contribute to immune escape, or those defining other variants designated as VOIs or VOCs, primarily arose in the S region. This observation aligns with findings from other studies [7,19,21].

Moreover, previous studies have identified numerous hotspot mutations within the SARS-CoV-2 genome, including S:HV69-70Del, S:Y144Del, and S:L452R, which have emerged with higher frequency than others [62,63]. In this study, patient E acquired two nonsynonymous hotspot mutations, S:HV69-70Del and S:L452R, and patient I acquired one hotspot mutation, S:Y144Del. All of these three hotspot mutations are the defining mutations of other major SARS-CoV-2 variants [3]. While the mutations S:S408R, S:T547K, and S:R493Q were observed in more than one patient, none of these were previously reported as hotspot mutations. However, both S:T547K and S:R493Q are also defining mutations of Omicron subvariants [3].

Of the 28 nonsynonymous mutations observed in the S region

of SARS-CoV-2 genomes, 12 were reported to be associated with immune evasion according to previous studies. S:G446D is a mutation in the receptor binding domain (RBD) and is associated with greatly reduced susceptibility to bebtelovimab and other monoclonal antibodies against SARS-CoV-2 [24,45], while S:D405N is a mutation that reduces the effects of sarbecovirus-neutralizing antibodies and is the defining mutations of omicron variants A.2, BA.2.12.1, BA.2.75, BA.4, BA.5, BQ.1, XBB, and XBB.1.5 [29]. S:K147E is the characteristic mutation of the BA.2.75 variant located in the N-terminal domain of the S region and confers resistance to polyclonal sera or monoclonal antibodies including bebtelovimab [46]. S:R408S is the defining mutation of several omicron subvariants, BA.2, BA.2.12.1, BA.2.75, BA.4, BA.5, BQ.1, XBB, and XBB.1.5 and might affect the conformation of RBD, causing decreased susceptibility to monoclonal antibodies [47]. S:L452R is a unique mutation of the omicron subvariants BA.4, BA.5, and BQ.1, located in the RBD, and confers escape from human leukocyte antigen-restricted cellular immunity [28]. S:V483A occupies the receptor binding motif and decreases viral susceptibility to monoclonal antibodies such as Bamlanivimab [48]. S:V445F is a mutation in the RBD and has been reported in other immunocompromised patients [22]. It also confers resistance to monoclonal antibodies [49].

S:HV69-70Del, S:Y144Del, and S:AL243-244Del are in the recurrent deletion region of the spike tip and contribute to resistance to some monoclonal antibodies [50], and S:H505Y has been reported to be associated with evasion from BA.1-specific neutralizing antibodies [29]. Lastly, S:L452Q is the specific mutation of the Lambda variant, located in the RBD, and confers decreased susceptibility to convalescent plasma and vaccines [31]. Also, the BA.2.12.1 Omicron subvariants carry it as their defining mutation. When patients got a booster vaccination with Comirnaty® against SARS-CoV-2, the neutralizing antibody response to BA.2.12.1 is less effective than to BA.1 or BA.2 [25].

Furthermore, out of 28 mutations in the S region, eleven were defining mutations of the major variants. Mutations characteristic of BA.4, BA.5, BA.2.75, BQ.1, XBB, XBB.1.5, and XBB.1.16 were identified in the SARS-CoV-2 genomes from these patients. Similar phenomena were observed in previous studies conducted during the pre-Omicron era, which documented the advent of mutations defining the Beta, Delta, or Omicron variants [2,3]. These findings could suggest that persistent viral detection in immunocompromised patients might contribute to the intra-host evolution of SARS-CoV-2. Therefore, monitoring these mutations might offer insights into the adaptation of SARS-CoV-2 and the

emergence of new variants.

Unlike the emergence of mutations associated with immune evasion, mutations related to antiviral resistance have not been extensively studied [9–11]. Their emergence is quite rare, less frequently than 0.001% among over six million sequences of *nsp12*–RdRP [64]. Moreover, there is evidence that viruses harboring some of these mutations replicated slowly and inefficiently [9,11]. However, some mutations associated with resistance to remdesivir have been reported. For example, the ORF1ab:V5184I (identical to NSP12–V792I) led to a 2.6–fold increase in the half–maximal effective concentration of remdesivir in vitro [11]. This mutation was identified in two patients with kidney transplants about one month after COVID–19 infection [10]. In this study, patient H acquired the same mutation on the 142nd day from the diagnosis of SARS–CoV–2 infection, after prolonged administration of remdesivir. The fitness cost and degree of remdesivir resistance of viruses carrying this mutation were not evaluated by experiments in patient H, so the clinical implications of NSP12–V792I warrant further investigation.

Both innate and adaptive immunity work in tandem to prevent, suppress, and eradicate SARS–CoV–2 infection. CD8+ T cells play crucial roles in mitigating the progression of COVID–19, but it’s primarily B cells and CD4+ T cells that are responsible for clearing

SARS-CoV-2 [65]. Instead of impaired T-cell immunity, B-cell depletion is considered the main factor extending the duration of SARS-CoV-2 shedding [38,65]. However, some reports suggested that SARS-CoV-2 infections were not effectively cleared despite the presence of high titers of neutralizing antibodies [7,66]. One patient in this study also continued to shed the virus from day 72 to day 79, though the patient had a high titer of neutralizing antibodies against the Omicron subvariant with which the patient was infected. This could be attributed to weakened CD4+ T cell immunity or changes in the sensitivity of SARS-CoV-2 to neutralizing antibodies, resulting from the accumulation of mutations that provided the virus with an ability to evade the immune responses [7,67]. WGS analyses demonstrated that the S:L452Q mutation, known for its association with immune evasion, appeared on day 79 and disappeared on day 98 in specimens from this patient. Although the exact duration of the S:L452Q and the status of T cell immunity in this patient could not be precisely determined, the persistent viral shedding from day 72 to day 79, despite the high titers of neutralizing antibodies, might be related to the S:L452Q mutation.

The emergence of new mutations was observed in the specimens, even those with a negative SARS-CoV-2 culture result. This observation suggests that a negative result from a viral culture

does not necessarily imply the absence of replication-competent viruses [68-70]. The sensitivity of viral culture for detecting SARS-CoV-2 shedding may be low. Additionally, the sampling and storage procedures of specimens might influence the yields of viral cultures [68,69]. The integrity of viral genomes and the presence of neutralizing antibodies bound to the viruses could also reduce the recovery of replication-competent viruses in culture [69,70]. Therefore, mutations could accumulate in the SARS-CoV-2 genome and viable viruses could be shed from immunocompromised patients, even when the results of viral culture are negative [68].

This study has several limitations. First, we did not perform WGS analyses on all the samples obtained from the patients. Consequently, we could not determine the precise durations for which specific mutations were present. Second, we could not collect samples from the patients at regular intervals. Thus, the frequency and interval of sample collection varied among the patients, potentially leading to more mutations being detected in patients with more samples. Third, we used both saliva and nasopharyngeal swab samples for viral culture, as the sequential collection of nasopharyngeal swabs posed greater challenges than saliva collection. Previous research has suggested that saliva samples may be less effective than nasopharyngeal swabs for SARS-CoV-2

culture [71], so this study may have underestimated the duration of persistent viral shedding in immunocompromised patients. Lastly, we did not assess the status of T-cell immunity in these patients. Therefore, the influence of T-cell immunity on viral shedding and the fixation of new mutations was not considered. Nevertheless, the majority of T-cell epitopes, about 80-90%, are conserved in the Omicron variants, and T-cell responses against SARS-CoV-2 depend on the repertoire of human leukocyte antigen (HLA) class I alleles. Changes in HLA haplotype can affect T-cell responses [72,73]. Therefore, making definitive conclusions about T-cell responses could be challenging without data on the distribution of HLA haplotypes and the results of stimulation assays between HLA class I alleles and T-cell epitopes in the SARS-CoV-2 variants.

# Chapter V. Conclusion

Several new mutations reported to be associated with immune evasion, remdesivir resistance, and the newly emerged variants such as BA.2.75, BA.4, BA.5, BQ.1, and XBB, emerged in the SARS-CoV-2 genomes of immunocompromised patients with persistent viral detection during the Omicron-prevalent era. Regarding the emergence of new strains with mutations reported to be related to immune evasion or remdesivir resistance and the possibility of shedding viable viruses from immunocompromised individuals, decisions to end the isolation of immunocompromised patients with SARS-CoV-2 infection should be made with caution.

# Bibliography


1. World Health Organization. WHO Coronavirus (COVID-19) Dashboard. 2023. Available at: https://covid19.who.int/. Accessed 14 April 2023.

2. World Health Organization. Updated working definitions and primary actions for SARS-CoV-2 variants. 2023. Available at: https://www.who.int/publications/m/item/updated-working-definitions-and-primary-actions-for--sars-cov-2-variants. Accessed 27 June 2023.

3. Emma Hodcroft. CoVariants. 2023. Available at: https://covariants.org/. Accessed 14 April 2023.

4. Centers for Disease Control and Prevention. SARS-CoV-2 variant classifications and definitions. 2023. Available at: https://www.cdc.gov/coronavirus/2019-ncov/variants/variant-classifications.html. Accessed 14 April 2023.

5. Karyakarte RP, Das R, Dudhate S, et al. Clinical characteristics and outcomes of laboratory-confirmed SARS-CoV-2 cases infected with Omicron subvariants and the XBB recombinant variant. Cureus 2023; 15:e35261.

6. Uraki R, Iida S, Halfmann PJ, et al. Characterization of SARS-CoV-2 Omicron BA.2.75 clinical isolates. Nat Commun 2023; 14:1620.

7. Sonnleitner ST, Prelog M, Sonnleitner S, et al. Cumulative SARS-CoV-2 mutations and corresponding changes in immunity in an immunocompromised patient indicate viral evolution within the host. Nat Commun 2022; 13:2560.

8. Leung WF, Chorlton S, Tyson J, et al. COVID-19 in an immunocompromised host: persistent shedding of viable SARS-CoV-2 and emergence of multiple mutations: a case report. Int J Infect Dis 2022; 114:178–182.

9. Gandhi S, Klein J, Robertson AJ, et al. De novo emergence of a remdesivir resistance mutation during treatment of persistent SARS-CoV-2 infection in an immunocompromised patient: a case report. Nat Commun 2022; 13:1547.

10. Hogan JI, Duerr R, Dimartino D, et al. Remdesivir resistance in transplant recipients with persistent coronavirus disease 2019. Clin Infect Dis 2023; 76:342–345.

11. Stevens LJ, Pruijssers AJ, Lee HW, et al. Mutations in the SARS-CoV-2 RNA-dependent RNA polymerase confer resistance to remdesivir by distinct mechanisms. Sci Transl Med 2022; 14:eabo0718.

12. Aydillo T, Gonzalez-Reiche AS, Aslam S, et al. Shedding of viable SARS-CoV-2 after immunosuppressive therapy for cancer. N Engl J Med 2020; 383:2586–2588.

13. Choi B, Choudhary MC, Regan J, et al. Persistence and evolution of SARS-CoV-2 in an immunocompromised host. N Engl J Med 2020; 383:2291–2293.

14. Weigang S, Fuchs J, Zimmer G, et al. Within-host evolution of SARS-CoV-2 in an immunosuppressed COVID-19 patient as a source of immune escape variants. Nat Commun 2021; 12:6405.

15. Hettle D, Hutchings S, Muir P, Moran E. Persistent SARS-CoV-2 infection in immunocompromised patients facilitates rapid viral evolution: Retrospective cohort study and literature review. Clin Infect Pract 2022; 16:100210.

16. Morishita M, Suzuki M, Matsunaga A, et al. Prolonged SARS-CoV-2 infection associated with long-term corticosteroid use in a patient with impaired B-cell immunity. J Infect Chemother 2022; 28:971–974.

17. Yousaf M, Hameed M, Alsoub H, Khatib M, Jamal W, Ahmad M. COVID-19: Prolonged viral shedding in an HIV patient with literature review of risk factors for prolonged viral shedding and its implications for isolation strategies. Clin Case Rep 2021; 9:1397–1401.

18. Benotmane I, Risch S, Doderer-Lang C, Caillard S, Fafi-Kremer S. Long-term shedding of viable SARS-CoV-2 in kidney transplant recipients with COVID-19. Am J Transplant 2021; 21:2871–2875.

19. Borges V, Isidro J, Cunha M, et al. Long-term evolution of SARS-CoV-2 in an immunocompromised patient with non-hodgkin lymphoma. mSphere 2021; 6:e0024421.

20. Chaguza C, Hahn AM, Petrone ME, et al. Accelerated SARS-CoV-2 intrahost evolution leading to distinct genotypes during chronic infection. Cell Rep Med 2023; 4:100943.

21. Pérez-Lago L, Aldámiz-Echevarría T, García-Martínez R, et al. Different within-host viral evolution dynamics in severely immunosuppressed cases with persistent sars-cov-2. Biomedicines 2021; 9:808.

22. Ko KKK, Yingtaweesittikul H, Tan TT, et al. Emergence of SARS-CoV-

2 spike mutations during prolonged infection in immunocompromised hosts. Microbiol Spectr 2022; 10:e0079122.

23. Baek YJ, Park G, Choi JY, et al. Within-host evolution of SARS-CoV-2 in a B-cell depleted patient with successful treatment. J Korean Med Sci 2023; 38:e175.

24. Liu Z, VanBlargan LA, Bloyet LM, et al. Identification of SARS-CoV-2 spike mutations that attenuate monoclonal and serum antibody neutralization. Cell Host Microbe 2021; 29:477-488.e4.

25. Hachmann NP, Miller J, Collier AY, et al. Neutralization escape by SARS-CoV-2 Omicron subvariants BA.2.12.1, BA.4, and BA.5. N Engl J Med 2022; 387:86–88.

26. Wang M, Zhang L, Li Q, et al. Reduced sensitivity of the SARS-CoV-2 Lambda variant to monoclonal antibodies and neutralizing antibodies induced by infection and vaccination. Emerg Microbes Infect 2022; 11:18–29.

27. Snell LB, Alcolea-Medina A, Charalampous T, et al. Real-time whole genome sequencing to guide patient-tailored therapy of severe acute respiratory syndrome coronavirus 2 infection. Clin Infect Dis 2023; 76:1125–1128.

28. Motozono C, Toyoda M, Zahradnik J, et al. SARS-CoV-2 spike L452R variant evades cellular immunity and increases infectivity. Cell Host Microbe 2021; 29:1124-1136.e11.

29. Cao Y, Yisimayi A, Jian F, et al. BA.2.12.1, BA.4 and BA.5 escape antibodies elicited by Omicron infection. Nature 2022; 608:593–602.

30. Kimura I, Kosugi Y, Wu J, et al. The SARS-CoV-2 Lambda variant exhibits enhanced infectivity and immune resistance. Cell Rep 2022; 38:110218.

31. Guo H, Fan Q, Song S, et al. Increased resistance of SARS-CoV-2 Lambda variant to antibody neutralization. J Clin Virol 2022; 150–151:105162.

32. Kokic G, Hillen HS, Tegunov D, et al. Mechanism of SARS-CoV-2 polymerase stalling by remdesivir. Nat Commun 2021; 12:279.

33. Kemp SA, Collier DA, Datir RP, et al. SARS-CoV-2 evolution during treatment of chronic infection. Nature 2021; 592:277–282.

34. Buckland MS, Galloway JB, Fhogartaigh CN, et al. Treatment of COVID-19 with remdesivir in the absence of humoral immunity: a case

report. Nat Commun 2020; 11:6385.

35. Centers for Disease Control and Prevention. 'People who are immunocompromised'. Available at: https://www.cdc.gov/coronavirus/2019-ncov/need-extra-precautions/people-who-are-immunocompromised.html. Accessed 8 April 2023.

36. Han MS, Byun JH, Cho Y, Rim JH. RT-PCR for SARS-CoV-2: quantitative versus qualitative. Lancet Infect Dis 2021; 21:165.

37. Kim H, Yang JS, Ko JH, et al. Can nirmatrelvir/ritonavir treatment shorten the duration of COVID-19 isolation? Front Med (Lausanne) 2022; 9:988559.

38. Kang SW, Kim JW, Kim JY, et al. Characteristics and risk factors of prolonged viable virus shedding in immunocompromised patients with COVID-19: a prospective cohort study. J Infect 2023; 86:412–414.

39. Kim C, Ryu DK, Lee J, et al. A therapeutic neutralizing antibody targeting receptor binding domain of SARS-CoV-2 spike protein. Nat Commun 2021; 12:288.

40. Noh JY, Yang JS, Hwang SY, et al. Duration of humoral immunity and cross-neutralizing activity against the Alpha, Beta, and Delta variants after wild-type severe acute respiratory syndrome coronavirus 2 infection: A prospective cohort study. J Infect Dis 2022; 226:975–978.

41. Cohen BJ, Audet S, Andrews N, Beeler J. Plaque reduction neutralization test for measles antibodies: Description of a standardised laboratory method for use in immunogenicity studies of aerosol vaccination. Vaccine 2007; 26:59–66.

42. The National Institutes of Health. Coronavirus disease 2019 treatment guidelines. 2023. Available at: https://www.covid19treatmentguidelines.nih.gov/. Accessed 27 June 2023.

43. Hadfield J, Megill C, Bell SM, et al. NextStrain: Real-time tracking of pathogen evolution. Bioinformatics 2018; 34:4121–4123.

44. Hodcroft E, Neher R. Phylogenetic analysis of SARS-CoV-2 clusters in their international context. 2023. Available at: https://nextstrain.org/groups/neherlab/ncov. Accessed 27 June 2023.

45. Ordaya EE, Vergidis P, Razonable RR, Yao JD, Beam E. Genotypic and predicted phenotypic analysis of SARS-COV-2 Omicron subvariants in immunocompromised patients with COVID-19 following tixagevimab-

cilgavimab prophylaxis. J Clin Virol 2023; 160:105382.

46. Wang Q, Iketani S, Li Z, et al. Antigenic characterization of the SARS-CoV-2 Omicron subvariant BA.2.75. Cell Host Microbe 2022; 30:1512-1517.e4.

47. Zhou H, Dcosta BM, Landau NR, Tada T. Resistance of SARS-CoV-2 Omicron BA.1 and BA.2 variants to vaccine-elicited sera and therapeutic monoclonal antibodies. Viruses 2022; 14:1334.

48. Lennerstrand J, Palanisamy N. Global prevalence of adaptive and prolonged infections' mutations in the receptor-binding domain of the sars-cov-2 spike protein. Viruses 2021; 13:1974.

49. Starr TN, Greaney AJ, Addetia A, et al. Prospective mapping of viral mutations that escape antibodies used to treat COVID-19. Science 2021; 371:850–854.

50. McCarthy KR, Rennick LJ, Nambulli S, et al. Recurrent deletions in the SARS-CoV-2 spike glycoprotein drive antibody escape. Science 2021; 371:1139–1142.

51. Kirchdoerfer RN, Ward AB. Structure of the SARS-CoV nsp12 polymerase bound to nsp7 and nsp8 co-factors. Nat Commun 2019; 10:2342.

52. Fumagalli SE, Padhiar NH, Meyer D, et al. Analysis of 3.5 million SARS-CoV-2 sequences reveals unique mutational trends with consistent nucleotide and codon frequencies. Virol J 2023; 20:31.

53. Cushing A, Kamali A, Winters M, et al. Emergence of hemagglutinin mutations during the course of influenza infection. Sci Rep 2015; 5:16178.

54. Liu L, Zeng F, Rao J, et al. Comparison of clinical features and outcomes of medically attended COVID-19 and influenza patients in a defined population in the 2020 respiratory virus season. Front Public Health 2021; 9:587425.

55. Day T, Gandon S, Lion S, Otto S. On the evolutionary epidemiology of SARS-CoV-2. Curr Biol 2020; 30:R849–R857.

56. Rocha E, Cox NJ, Black RA, Harmon MW, Harrison CJ, Kendal' AP. Antigenic and genetic variation in Influenza A (HINI) virus isolates recovered from a persistently infected immunodeficient child. J Virol 1991; 65:2340–2350.

57. Liu J, Zhang S, Dong X, et al. Corticosteroid treatment in severe

COVID-19 patients with acute respiratory distress syndrome. J Clin Invest 2020; 130:6417–6428.

58. Heyer A, Günther T, Robitaille A, et al. Remdesivir-induced emergence of SARS-CoV2 variants in patients with prolonged infection. Cell Rep Med 2022; 3:100735.

59. Velazquez-Salinas L, Zarate S, Eberl S, Gladue DP, Novella I, Borca M V. Positive selection of ORF1ab, ORF3a, and ORF8 genes drives the early evolutionary trends of SARS-CoV-2 during the 2020 COVID-19 pandemic. Front Microbiol 2020; 11:550674.

60. Salles TS, Cavalcanti AC, da Costa FB, et al. Genomic surveillance of SARS-CoV-2 Spike gene by sanger sequencing. PLoS One 2022; 17:e0262170.

61. Gálvez JM, Chaparro-Solano HM, Pinzón-Rondón ÁM, et al. Mutation profile of SARS-CoV-2 genome in a sample from the first year of the pandemic in Colombia. Infect Genet Evol 2022; 97:105192.

62. Mullick B, Magar R, Jhunjhunwala A, Barati Farimani A. Understanding mutation hotspots for the SARS-CoV-2 spike protein using Shannon Entropy and K-means clustering. Comput Biol Med 2021; 138:104915.

63. Saha I, Ghosh N, Sharma N, Nandi S. Hotspot mutations in SARS-CoV-2. Front Genet 2021; 12:753440.

64. Focosi D, Maggi F, McConnell S, Casadevall A. Very low levels of remdesivir resistance in SARS-COV-2 genomes after 18 months of massive usage during the COVID19 pandemic: A GISAID exploratory analysis. Antiviral Res 2022; 198:105247.

65. DeWolf S, Laracy JC, Perales MA, Kamboj M, van den Brink MRM, Vardhana S. SARS-CoV-2 in immunocompromised individuals. Immunity 2022; 55:1779–1798.

66. Li L, Li S, Pan Y, et al. An immunocompetent patient with high neutralizing antibody titers who shed COVID-19 virus for 169 days — China, 2020. China CDC Wkly 2021; 3:688–691.

67. Müller K, Girl P, Giebl A, et al. Sensitivity of two SARS-CoV-2 variants with spike protein mutations to neutralising antibodies. Virus Genes 2021; 57:502–509.

68. Binnicker M. Can testing predict SARS-CoV-2 infectivity? The potential for certain methods to be surrogates for replication-competent virus. J Clin Microbiol 2021; 59:e0046921.

69. Gniazdowski V, Paul Morris C, Wohl S, et al. Repeated coronavirus disease 2019 molecular testing: correlation of severe acute respiratory syndrome coronavirus 2 culture with molecular assays and cycle thresholds. Clin Infect Dis 2021; 73:E860–E869.

70. Huang CG, Lee KM, Hsiao MJ, et al. Culture-based virus isolation to evaluate potential infectivity of clinical specimens tested for COVID-19. J Clin Microbiol 2020; 58:e01068-20.

71. Tallmadge RL, Laverack M, Cronk B, et al. Viral RNA load and infectivity of SARS-CoV-2 in paired respiratory and oral specimens from symptomatic, asymptomatic, or postsymptomatic individuals. Microbiol Spectr 2022; 10:e0226421.

72. Choi SJ, Kim DU, Noh JY, et al. T cell epitopes in SARS-CoV-2 proteins are substantially conserved in the Omicron variant. Cell Mol Immunol 2022; 19:447–448.

73. Tarke A, Sidney J, Kidd CK, et al. Comprehensive analysis of T cell immunodominance and immunoprevalence of SARS-CoV-2 epitopes in COVID-19 cases. Cell Rep Med 2021; 2:100204.

# 국 문 초 록

**배경:** 2019년 12월 중증 급성 호흡기 증후군-코로나바이러스-2가 (SARS-CoV-2) 처음 등장한 이후로, 여러 가지 관심 변이종과 주요 변이종이 발생했다. SARS-CoV-2는 면역저하 환자 체내에서 장기간 존속하면서 새로운 변이를 획득할 수 있고, 이로 인해 면역 회피 또는 치료에 내성을 지니는 새로운 변이종이 출현할 수 있다. 따라서, 새로운 돌연변이들의 동태, 특성, 그리고 임상적 영향을 이해하기 위해서 이러한 변이들을 감시하는 것이 필요하다. 대다수의 이전 연구들은 오미크론 유행 전에 수행됐고 소수의 면역저하자만 포함했으며, 면역 회피와 관련된 변이를 중점적으로 확인했다. 이에 따라 오미크론이 유행하는 시기에 더 많은 수의 면역저하자를 포함해서, 새로운 돌연변이들의 특성을 포괄적으로 살펴보는 추가 연구가 필요하다. 본 연구는, 오미크론이 유행하는 시기에 면역저하자에서 축적되는 SARS-CoV-2 비동의적 변이의 특성을 조사하고자 한다.

**방법:** 본 전향 연구는 SARS-CoV-2에 처음 감염된 성인 면역저하자를 대상으로 2022년 2월부터 11월까지 수행됐다. 가능한 한 환자로부터 주 1회 침, 가래, 그리고 혈액을 수집했고 유전체 및 항체 검사를 시행했다. 중합효소 연쇄 반응을 통해 SARS-CoV-2 RNA의 양을 측정했고, 실시간 역전사 중합효소 연쇄 반응 결과 양성이 확인된 검체로 바이러스

를 배양했다. 또한 호흡기 검체로 전체 유전체 시퀀싱을 (WGS) 수행하고 새로운 변이를 초래하는 핵산 염기 다형성을 식별하고 분류했다. 문헌 고찰을 통해 확인된 변이가 면역 회피, 렘데시비르 내성, 또는 다른 SARS-CoV-2 변이종과 관련이 있는지 조사했다. 또한, 혈액 검체로 플라크 감소 중화 검사를 시행해 SARS-CoV-2 오미크론 변이종에 대한 중화 항체 역가를 측정했다.

**결과:** 최종 분석에 13명의 환자들이 포함됐는데, 이 중 11명은 (84.6%) 혈액 종양 환자였고 2명은 (15.4%) 고형장기 이식 환자였다. 절반 정도의 환자가 (46.2%) SARS-CoV-2 진단 전 2년 이내에 B세포를 제거하는 치료제를 맞았고, 환자 두 명만이 (15.4%) SARS-CoV-2 백신을 최소 세 번 접종 받았다. 또한 9명의 환자들이 (69.2%) BA.2 또는 BA.2.3 오미크론 하위 계통에 감염됐다.

WGS 분석은 중앙값으로 세 번 정도 각 면역저하 환자에서 시행됐고, 분석 간 간격의 중앙값은 20일이었다. 또한 환자들의 첫 분석과 마지막 분석 사이 간격의 중앙값은 51일이었다. 환자들은 중앙값으로 2개 정도의 비동의적 돌연변이를 획득했고, 이 변이들은 바이러스 유전체 전체에 퍼져 있었다. 총 87개의 비동의적 변이 중 16개와 (18.3%) 13개가 (14.9%) 지속 변이와 일시 변이로 분류됐고, 대부분은 ORF1ab 영역에 있었다. 돌기 영역에서는 28개의 변이가 확인됐는데, 이 중 12개가 면역 회피와 연관됐고, 11개는 BA.1, BA.4, BA.5, BA.2.75, XBB, 그리고 XBB.1.5와 같은 오미크론 하위 변이종을 포함한 다른 변이종들

의 정의 변이였다. 다른 변이종에서 확인되는 정의 변이 비율은, 돌기 영역에서 전체 유전체에 비해 더 높았다. (39.3% vs. 14.9%)

환자 H는 SARS-CoV-2 진단 후 142일 뒤 렘데시비르에 대한 감수성 감소와 관련된 것으로 보고된 변이 ORF1ab:V5184I를 획득했다. 이 환자는 이 변이가 나타나기 전 여러 차례에 걸쳐 렘데시비르, 덱사메타손, 그리고 바리시티닙을 투약 받았고, 고용량 스테로이드를 두 달 이상 사용했다. 환자 J는 높은 역가의 중화항체를 보유했음에도 불구하고, 바이러스를 계속적으로 배출했다. 이는 면역 회피와 중화항체 감수성 감소와 관련된 것으로 보고된 비동의적 변이 S:L452Q 때문일 수 있다.

**결론:** 오미크론 유행 시기에 바이러스가 지속적으로 검출되는 면역저하자들의 SARS-CoV-2 유전체에서, 면역 회피, 렘데시비르 저항성, 그리고 BA.2.75, BA.4, BA.5, BQ.1, XBB와 같은 새로운 오미크론 하위 변이종과 관련된 것으로 보고된 여러 새로운 변이들이 발견됐다. 면역 회피 또는 렘데시비르 저항성과 관련된 변이를 가진 새로운 변이종의 등장과 면역저하자들로부터 바이러스가 지속적으로 배출될 가능성을 고려하면, SARS-CoV-2에 감염된 면역저하자들을 격리 해제하기 위해서는 신중하게 검토해야 한다.

**키워드: 중증급성호흡기증후군 코로나바이러스-2, 면역억제, 전체 유전체 시퀀싱, 비동의적 돌연변이, 면역 회피성, 렘데시비르 저항성**